ARTICLE

doi:10.1038/nature12647

A regenerative approach to the treatment of multiple sclerosis

Vishal A. Deshmukh[1], Virginie Tardif[2], Costas A. Lyssiotis[1]†, Chelsea C. Green[1], Bilal Kerman[3], Hyung Joon Kim[3], Krishnan Padmanabhan[3], Jonathan G. Swoboda[1], Insha Ahmad[1], Toru Kondo[4], Fred H. Gage[3], Argyrios N. Theofilopoulos[2], Brian R. Lawson[2]*, Peter G. Schultz[1,5]* & Luke L. Lairson[1,5]*

Progressive phases of multiple sclerosis are associated with inhibited differentiation of the progenitor cell population that generates the mature oligodendrocytes required for remyelination and disease remission. To identify selective inducers of oligodendrocyte differentiation, we performed an image-based screen for myelin basic protein (MBP) expression using primary rat optic-nerve-derived progenitor cells. Here we show that among the most effective compounds identifed was benztropine, which significantly decreases clinical severity in the experimental autoimmune encephalomyelitis (EAE) model of relapsing-remitting multiple sclerosis when administered alone or in combination with approved immunosuppressive treatments for multiple sclerosis. Evidence from a cuprizone-induced model of demyelination, *in vitro* and *in vivo* T-cell assays and EAE adoptive transfer experiments indicated that the observed efficacy of this drug results directly from an enhancement of remyelination rather than immune suppression. Pharmacological studies indicate that benztropine functions by a mechanism that involves direct antagonism of M1 and/or M3 muscarinic receptors. These studies should facilitate the development of effective new therapies for the treatment of multiple sclerosis that complement established immunosuppressive approaches.

Remyelination persists throughout adulthood in the central nervous system and involves the generation of new myelinating oligodendrocytes[1]. Despite some controversy regarding their intrinsic *in vitro* and *in vivo* lineage potential[2–4], compelling evidence indicates that a widespread proliferating population of nerve and glial antigen-2 (NG2), platelet-derived growth factor receptor alpha (PDGFR-α) positive cells, termed NG2-glia or oligodendrocyte precursor cells (OPCs), are the major source of newly formed mature oligodendrocytes required for remyelination[5–7]. Remission in multiple sclerosis is largely dependent on migration of OPCs to sites of injury and subsequent differentiation to mature cells capable of repair[1,2,8]. Studies evaluating the presence and relative densities of OPCs at sites of chronically demyelinated multiple sclerosis lesions indicate that it is not a failure of repopulation or migration of OPCs, but rather inhibition of OPC differentiation at sites of injury that contributes to disease progression[9–12]. As such, the identification of small molecules that selectively induce differentiation of OPCs at sites of demyelinated lesions and thereby enhance remyelination would have a considerable impact on the development of new effective treatments for multiple sclerosis[13].

High-throughput OPC differentiation screen

To identify drug-like small molecules that selectively induce OPC differentiation, we developed a high content imaging assay based on the induction of MBP expression in primary rat optic nerve-derived OPCs cultured for 6 days under basal differentiation conditions. Primary rodent OPCs proliferate *in vitro* when cultured in serum-free media containing PDGF-AA[14]. Upon withdrawal of PDGF-AA, immature $A2B5^+$ OPCs cease to proliferate, but also fail to efficiently differentiate into MBP producing mature oligodendrocytes. Addition of thyroid hormone (triiodothyronine; T3), a known inducer of OPC differentiation[15–19], at the time of mitogen withdrawal results in the differentiation of OPCs to MBP-positive oligodendrocytes after 6 days of culture (Extended Data Fig. 1a). However, T3 has several physiological effects that make it unattractive as a therapeutic agent for multiple sclerosis. This assay was adapted to a high-throughput format and used to screen a collection of ~100,000 structurally diverse molecules (Extended Data Fig. 1b). This led to the identification of several previously identified inducers of OPC differentiation[19–23] (Extended Data Fig. 1c, summarized in Supplementary Table 1). Unfortunately, these molecules have limited therapeutic potential due to off-target activities, toxicity, poor brain exposure and/or demonstrated lack of *in vivo* efficacy. Among the most effective inducers of OPC differentiation was benztropine (half-maximum effective concentration (EC_{50}) ~500 nM) (Fig. 1a and Extended Data Fig. 2a, b), which we chose to investigate further because it is an orally available approved drug that readily crosses the blood–brain barrier.

Benztropine-induced *in vitro* differentiation of rodent OPCs was confirmed by evaluating the transcription and translation levels of the oligodendrocyte-specific markers MBP and myelin oligodendroglial glycoprotein (MOG) by western blot and quantitative polymerase chain reaction with reverse transcription (qRT–PCR) analysis (Extended Data Fig. 2c, d). Additionally, *in vitro* OPC differentiation activity was confirmed by immunofluorescence analysis using multiple markers specifically expressed in mature oligodendrocytes following 6 days of compound treatment (Extended Data Fig. 2e). Furthermore, transcript levels of cyclin D1, cyclin D2, *c-Fos* and *c-Jun* were significantly decreased in benztropine-treated OPCs, consistent with general inhibition of cell cycle progression (Extended Data Fig. 2f). To determine the stage of OPC differentiation at which benztropine is active[24,25], we treated OPCs for differing durations starting at several time points (Extended Data Fig. 2g, h). Maximal induction of MBP expression

[1]Department of Chemistry, The Scripps Research Institute, 10550, North Torrey Pines Road, La Jolla, California 92037, USA. [2]Department of Immunology and Microbial Science, The Scripps Research Institute, 10550 North Torrey Pines Road, La Jolla, California 92037, USA. [3]Laboratory of Genetics, The Salk Institute for Biological Sciences, 10010 North Torrey Pines Road, La Jolla, California 92037, USA. [4]Division of Stem Cell Biology, Institute for Genetic Medicine, Hokkaido University, Kita-15, Nishi- 7, Kita-ku, Sapporo 060-0815, Japan. [5]The California Institute for Biomedical Research, 11119 North Torrey Pines Road, La Jolla, California 92037, USA. †Present Address: Weill Cornell Medical College, 1300 York Avenue, New York, New York 10065, USA.
*These authors contributed equally to this work.

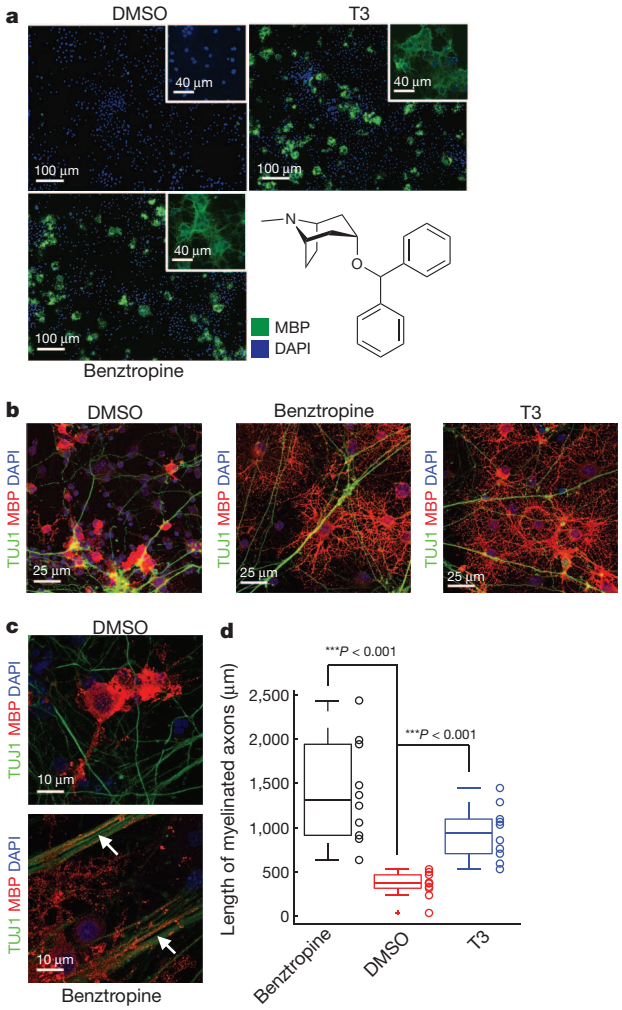

Figure 1 | Benztropine induces oligodendrocyte precursor cell differentiation and *in vitro* myelination of co-cultured axons. **a**, Benztropine (1.5 μM)- and T3 (1.0 μM)-treated rat OPCs immunostained for MBP (green) and 4′,6-diamidino-2-phenylindole (DAPI, blue). Structure of benztropine. **b**, Benztropine (1.0 μM)- and T3 (1.0 μM)-treated co-culture of mouse embryonic-stem-derived neurons with rat OPCs immunostained for TUJ1 (tubulin marker, axons), MBP (oligodendrocytes) and DAPI (nuclei). **c**, Effect of benztropine (1.0 μM) treatment on the myelination of axons. Arrows denote myelinated axons. **d**, Quantification of total axonal myelination in OPC with neuron co-cultures ($n = 10$, mean and s.e.m., $^{***}P < 0.001$, ANOVA with Bonferroni correction).

was observed when the compound was added within 48 h of PDGF-AA withdrawal and cells were further cultured for at least 5 days, indicating that this drug probably acts on immature A2B5$^+$ OPCs and not the intermediate 'pre-oligodendrocyte' stage of differentiation.

Benztropine was also found to induce robust differentiation of rat and mouse OPCs when co-cultured with mouse embryonic-stem-cell-derived neurons[26] or mouse cortex-derived cells[27] (Fig. 1b and Extended Data Fig. 3a, b, respectively). We also quantified the effect of benztropine on the *in vitro* myelination of axons by quantifying the co-localization of MBP positive oligodendrocyte processes and axons (Extended Data Fig. 3c). The results showed a significant increase in the absolute amount of myelination in benztropine-treated co-cultures (Fig. 1c, d). This increase could result from enhanced maturation of oligodendrocytes and/or may reflect elevated myelination capacity of mature oligodendrocytes. To evaluate these two possibilities, we normalized the absolute amount of myelin to the total number of oligodendrocytes. Benztropine treated cultures had a significantly higher percentage of myelinating oligodendrocytes (Extended Data Fig. 3d), which indicates that benztropine not only enhances maturation of oligodendrocytes, but also promotes myelination.

M1/M3 muscarinic receptor antagonism

Benztropine is used clinically for the management of Parkinson's disease and its pharmacological effects are thought to result from its anticholinergic activity[28]. However, benztropine is also a centrally acting anti-histamine[29] and dopamine re-uptake inhibitor[30]. To determine which, if any, of these activities play a role in OPC differentiation, we evaluated the ability of selective agonists of muscarinic acetylcholine receptors (mAChRs) or nicotinic acetylcholine receptors (the agonists carbachol or nicotine, respectively) to block benztropine activity. Inhibition of benztropine-induced OPC differentiation was observed in the presence of carbachol (Extended Data Fig. 3e, f), whereas nicotine had no effect on OPC differentiation (Extended Data Fig. 3g). The dopamine receptor antagonist haloperidol, the dopamine receptor agonist quinpirole and the histaminergic receptor agonists histamine and histamine trifloromethyl-toluidine (HTMT) had no effect on benztropine-induced OPC differentiation (Extended Data Fig. 3h–k). Moreover, neither quinpirole nor nicotinic receptor antagonists (for example, tubocuraine, mivacurium, mecamylamine, pancuronium, atracurium or trimethophan) induced significant OPC differentiation (Extended Data Fig. 3l). We then evaluated a panel of mAChR antagonists (atropine, oxybutynin, scopolamine, ipratropium and propiverine) and found that all induced OPC differentiation in a dose-dependent manner with differing potencies (Supplementary Table 2), consistent with a mechanism of action that is dependent on muscarinic receptor antagonism.

To examine further the role of muscarinic receptor antagonism in benztropine-induced OPC differentiation and determine if a more potent and/or clinically useful drug could be identified, we evaluated a broader panel of structurally diverse muscarinic receptor antagonists. Of the 42 compounds tested, 20, which cluster amongst 4 related structural classes, were found to be active (Supplementary Tables 2 and 3). However, none were found to be more potent than benztropine. The ability of muscarinic receptor agonists to inhibit benztropine-induced OPC differentiation provides strong evidence that muscarinic receptor antagonism is an essential component of the mechanism of action. The inactivity of several of the muscarinic antagonists we evaluated could be the result of off-target inhibitory activities or toxicity-related effects. We cannot rule out the possibility that an additional biological activity, common among the active muscarinic receptor antagonists identified, is required for OPC differentiation. However, consistent with the proposed mechanism, it has recently been demonstrated that muscarinic activation causes decreased expression of myelin proteins in mature oligodendrocytes and modulates the expression of known regulators of differentiation (for example, PDFGRα) in immature OPCs[31]. Furthermore, Notch1 is a known negative regulator of OPC differentiation[32,33] and, consistent with the observation that muscarinic receptor activation causes increased expression of Notch1 (ref. 31), we found that treatment of OPCs with benztropine results in a significant decrease in Notch1 expression in immature OPCs (Extended Data Fig. 3m).

OPCs are known to express mAChRs, predominantly subtypes M1, M3 and M5 (ref. 34). We confirmed expression of these receptors, as well as that of the acetylcholine-synthesizing enzyme choline acetyl transferase (ChAT), by qRT–PCR (Extended Data Fig. 3n, o). Activation of mAChRs triggers protein-kinase-C-dependent activation of the MAPK/ERK pathway leading to modulation of c-Fos expression[35]. Western blot analysis of benztropine-treated OPCs is consistent with general inhibition of this pathway (decreased phospho-Akt and stimulated phosphorylation of p38 MAPK and CREB) (Extended Data Fig. 3p). Activation of M1 and M3 mAChRs is coupled to downstream signalling events through phospholipase C, which results in increased intracellular calcium concentrations[35], whereas M2 and M4 mAChR

activation inhibits adenylate cyclase, leading to decreased intracellular cAMP levels[31]. In OPCs, benztropine and the muscarinic antagonist atropine both inhibited carbachol-induced calcium influx (Extended Data Fig. 3q), but had no effect on cAMP levels (Extended Data Fig. 3r). Together, these results suggest that benztropine induces OPC differentiation by a mechanism involving direct antagonism of M1/M3 muscarinic receptors. Acetylcholine is a known regulator of OPC proliferation and, as such, muscarinic receptor subtypes represent a promising class of therapeutic targets for the modulation of OPC proliferation and differentiation[31–35].

Efficacy in the PLP-induced EAE model

We next examined the activity of benztropine in the proteolipid protein (PLP)-induced EAE rodent model of relapsing-remitting multiple sclerosis [36,37]. Despite some inherent limitations of this model, all therapies approved for the treatment of MS decrease the clinical severity of EAE[38,39]. This model is most commonly used to evaluate the potential efficacy of immunosuppressive agents, but can also be used to determine the effectiveness of promyelinating agents that function by enhancing OPC differentiation[40,41]. Benztropine (10 mg per kg) was administered prophylactically by a daily intraperitoneal (i.p.) injection regimen initiated at the onset of PLP immunization. Benztropine dramatically decreased the severity of the acute phase of disease and virtually eliminated the relapse phase compared to vehicle-treated controls (Fig. 2a and Extended Data Fig. 4a). We next evaluated efficacy

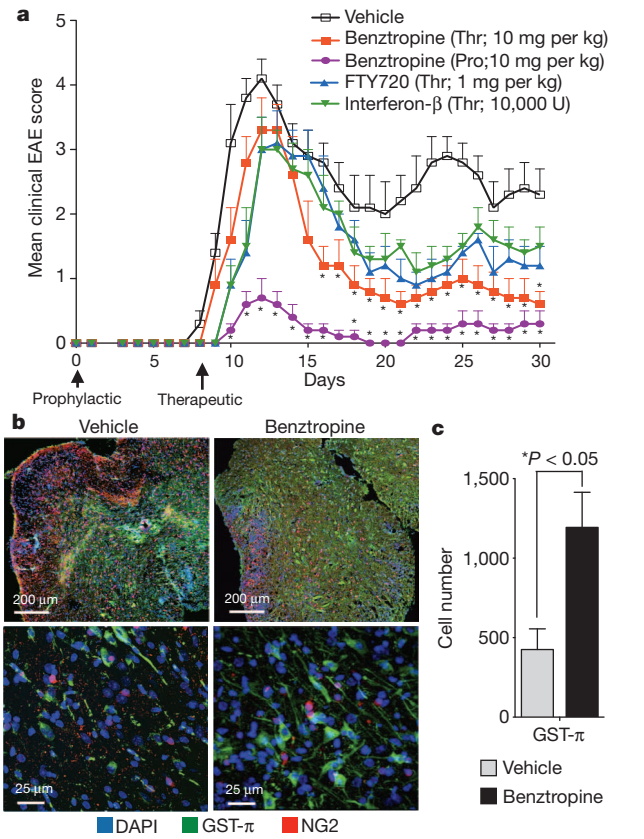

Figure 2 | Benztropine decreases disease severity in the PLP-induced EAE model. **a**, EAE severity scores (ranging from no observable disease to moribund/dead) following prophylactic (Pro, day 0) or therapeutic (Thr, time of initial symptoms) treatment with benztropine compared to therapeutically administered FTY720 or interferon-β ($n = 8$, mean and s.e.m., $^*P < 0.05$; t-test). **b**, Confocal images of spinal cord sections isolated at day 14 from EAE mice treated prophylactically with benztropine (10 mg per kg) or vehicle and immunostained for GST-π (mature oligodendrocytes) and NG2. **c**, Quantification of GST-π^+ cells ($n = 30$, mean and s.e.m., $^*P < 0.05$, t-test).

when the drug was administered therapeutically, by starting daily injections at the first sign of disease. Treatment with benztropine in this mode again led to functional recovery; significant decreases in clinical severity during remission phases were observed and the occurrence of relapse was again virtually eliminated (Fig. 2a). In fact, treatment with benztropine in this mode resulted in decreased clinical severity comparable to, or better than, that observed for the immunosuppressive multiple sclerosis drugs FTY720 or interferon-β (administered at reported therapeutic doses in mice) (Fig. 2a).

In parallel experiments, when benztropine was dosed in a prophylactic mode, we isolated spinal cords from drug- or vehicle-treated mice at various time points before the onset of symptoms and during the acute and relapse phases of disease. Sections from many regions were stained with Luxol fast blue to visualize myelin or Luxol fast blue and hematoxylin and eosin (H&E) to visualize both myelin and infiltrating immune cells. Immunohistochemical analysis was also performed using antibodies that recognize markers of mature oligodendrocytes (MBP and glutathione *S*-transferase; GST-π), immature OPCs (NG2) or infiltrating immune cells (CD45). During acute and relapse phases of disease, sections from both vehicle- and benztropine-treated mice showed significant infiltration by H&E- and CD45-positive immune cells (Extended Data Fig. 4b–d). In vehicle-treated mice, infiltration corresponded to areas of significant demyelination (Extended Data Fig. 4b, e). In contrast, in benztropine-treated mice, a large number of immune-cell-infiltrated areas stained positive for Luxol fast blue or MBP, a finding consistent with a regenerative versus immunosuppressive mechanism (Extended Data Fig. 4b, e). We further evaluated drug-enhanced remyelination using confocal microscopy (Fig. 2b). Quantitative image analysis of many random fields per group indicated that benztropine treatment caused a significant increase in the number of GST-π^+ mature oligodendrocytes from ~500 to ~1,100 per field compared to vehicle (Fig. 2c and Extended Data Fig. 4d). The observed increase in mature oligodendrocyte numbers is consistent with a mechanism of benztropine-induced clinical recovery that involves the stimulation of OPC differentiation, leading to enhanced remyelination, in the context of an inflammatory environment. Notably, at time points before any observable immune cell infiltration or disease onset (day 8), a similar (~twofold) increase in the number of mature oligodendrocyte was observed in the spinal cords of benztropine-treated mice (Extended Data Fig. 4c, d). This observation is consistent with the time frame of *in vitro* activity. Furthermore, it is consistent with the occurrence of benztropine-induced OPC differentiation *in vivo* in the absence of inflammatory insult and provides an explanation for the substantial decrease in clinical severity observed during the acute phase of disease when the drug is dosed in a prophylactic mode. Mature oligodendrocytes capable of remyelination are poised for repair (or possibly protection) before immunological attack. Importantly, general toxicity was not observed either microscopically or macroscopically in drug-treated mice following 4 weeks of daily injections at 10 mg per kg.

Electron microscopy was used to observe myelin surrounding spinal cord axons in benztropine- and vehicle-treated mice during the peak of the acute phase of disease. Immune-cell-infiltrated areas of spinal cords from vehicle-treated mice exhibited characteristic oligodendrogliopathy along with damaged axons with loose and separated layers of myelin sheaths[42] (Fig. 3a, b and Extended Data Fig. 4f). Benztropine treatment did not influence the infiltration or relative abundance of encephalogenic T cells and other inflammatory immune effector cells, nor did it affect the ability of these cells to cause demyelination during the acute phase of disease. Evidence for demyelination at this time point is provided by the significant ($P < 0.01$) increases in observed g-ratios (ratio of axon diameter to myelinated axon diameter) for both drug- and vehicle-treated mice compared to non-diseased controls (Fig. 3c and Extended Data Fig. 4g–i). Drug treatment resulted in extensive remyelination, as evidenced by the presence of abundant newly formed and notably thinner (compared to those of non-diseased mice) myelin sheaths (a characteristic associated with remyelination[5]) (Fig. 3a, b and

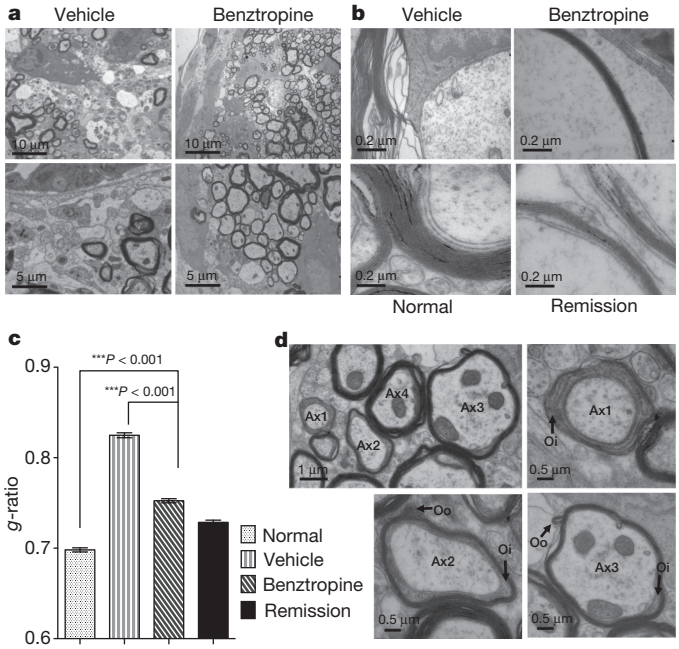

Figure 3 | Benztropine-induced remyelination in the PLP-induced EAE model. a, b, Electron microscopy images of spinal cords isolated from benztropine (Pro, 10 mg per kg)- and vehicle-treated EAE mice. **c**, *g*-ratios of spinal cord axons in normal and EAE mice ($n = 1{,}000$, mean and s.e.m., $***P < 0.001$, two-way ANOVA). **d**, Electron microscopy images of spinal cords isolated from benztropine-treated EAE mice highlighting different phases of remyelination (initial wrapping (Ax1), partial remyelination (Ax2), almost remyelinated (Ax3) and normal axon (Ax4)) and associated morphological features (outer (Oo) and inner (Oi) ends of cytoplasmic processes of oligodendrocytes wrapped around axons (Ax)).

Extended Data Fig. 4f). Specifically, the *g*-ratios in benztropine-treated mice were significantly lower ($P < 0.01$) than in vehicle-treated mice, yet still significantly higher ($P < 0.01$) than in non-diseased mice (Fig. 3c and Extended Data Fig. 4g–i). Moreover, in these areas, myelin sheaths were observed in different phases of remyelination (axons undergoing initial wrapping, partial remyelination and almost complete remyelination[42]) (Fig. 3d and Extended Data Fig. 4j), strongly supporting a benztropine-induced remyelination effect.

Effect on the immune system of EAE mice

The primary immunological processes involved in multiple sclerosis and EAE are thought to be T-cell mediated. To determine the extent to which the efficacy of benztropine in the EAE model results from T cell inhibitory activity, we evaluated the effects of benztropine and other muscarinic antagonists (atropine, oxybutynin, scopolamine, ipratropium and propiverine) on T-cell activation and proliferation. Notably, it has been reported that muscarinic receptors are expressed on T cells[43]. However, neither benztropine nor the other muscarinic antagonists had an effect on T-cell proliferation *in vitro*, as measured using a carboxyfluorescein succinimidyl ester (CFSE) labelling assay (Extended Data Fig. 5a), nor did they affect T-cell activation as determined by assessing $CD4^+CD69^+$ and $CD4^+CD25^+$ populations (Extended Data Fig. 5b, c). We also evaluated the effect of benztropine on the immune system *in vivo* in SJL/J mice in which EAE had or had not been induced with PLP. In both diseased and healthy animals, benztropine had no effect on the number of splenic naive ($CD44^{lo}$) or activated ($CD44^{Hi}$) $CD4^+$ and $CD8^+$ T cells (Extended Data Fig. 5d–f). A minor, but significant, decrease in B cell numbers was observed following treatment with benztropine (Extended Data Fig. 5e, f), and benztropine had no effect on cytokine (IL-2, IL-10, IFN-γ, TNF-α) producing T-cell populations isolated from drug- or vehicle-treated normal or diseased mice (Extended Data Fig. 5e, f). We also found that benztropine had no effect on antigen-induced IgG production (Extended Data Fig. 5g). Next, we analysed the effect of benztropine on *in vitro* macrophage development and M1/M2 polarization and observed no significant differences between benztropine-treated cultures and controls (Extended Data Fig. 6). Additionally, the expression of M1 or M2 polarization markers in spleens, spinal cords, as well as spinal-infiltrating leukocytes isolated from EAE mice treated with benztropine for 14 days, were equivalent to those of controls (Extended Data Fig. 7).

We next performed the adoptive transfer model of EAE[44] to further demonstrate that benztropine does not affect T-cell development or function. Splenocytes were isolated from SJL/J donor mice, following immunization with PLP and immediate daily injection with benztropine (10 mg per kg) or saline for 10 days, and then cultured *in vitro* in the presence of benztropine (5 µM) or vehicle, respectively (Extended Data Fig. 8). Injection of splenocytes from either donor group resulted in equally severe transfer of EAE disease to recipient mice (Extended Data Fig. 8: groups 1 and 3), providing evidence that benztropine had no effect on the development and function of PLP-specific T cells *in vivo* or *in vitro*. Benztropine (10 mg per kg) treatment of recipient mice, injected with splenocytes from vehicle- or benztropine-treated donor mice, resulted in significant reductions in clinical severity scores (Extended Data Fig. 8: groups 2 and 4) compared to controls (Extended Data Fig. 8: groups 1 and 3). Taken together, these results strongly suggest that the observed efficacy of benztropine in the EAE model results from remyelination arising from enhanced oligodendrogenesis rather than immune suppression.

Efficacy of benztropine in the cuprizone model

We further evaluated the ability of benztropine to induce OPC differentiation and enhance remyelination *in vivo* using the T-cell-independent cuprizone-induced model of demyelination. Inclusion of 0.2% (w/w) cuprizone in the diet of C57BL/6 mice induces a demyelination program that proceeds with a defined series of events over a characteristic time course in which the corpus callosum shows peak demyelination following 6–7 weeks[45]. Spontaneous remyelination is observed 2–4 weeks following cuprizone withdrawal[46]. By administering drugs when a cuprizone-free diet is reintroduced, the efficacy of promyelinating agents can be examined by evaluating the relative kinetics of OPC-dependent remyelination[45,46]. Upon withdrawal of cuprizone, we administered vehicle or benztropine (10 mg per kg) by daily i.p. injections for 5 weeks. During this time, mice were euthanized weekly and the degree of remyelination was quantitatively established by staining the corpus callosum regions of harvested brains with Luxol fast blue and anti-GST-π^+ antibody. Significant demyelination was clearly observed after seven weeks of cuprizone treatment compared to naive animals (Fig. 4a, top left and bottom left panels). Consistent with enhanced OPC differentiation and accelerated remyelination, overall myelin staining (Fig. 4a, middle and right panels; 4b; Extended Data Fig. 9) and the number of GST-π^+ mature oligodendrocytes (Fig. 4c, d) increased significantly in the corpus callosum at week 2 following benztropine treatment compared to the spontaneous remyelination observed in vehicle controls. As expected, at later time points, spontaneous remyelination was relatively complete and no significant differences between drug- and vehicle-treated animals were observed. A lack of difference at these later time points indicates that, even after five weeks of treatment, benztropine is not toxic to mature oligodendrocytes. These data again indicate that benztropine enhances the process of *in vivo* remyelination by directly inducing OPC differentiation.

Benztropine is dose-sparing with FTY720

For the treatment of multiple sclerosis, an OPC differentiation-inducing drug would most probably be introduced clinically as part of a combination therapy with an immunosuppressive drug. Using the PLP-induced EAE model, we therefore evaluated the clinical efficacy of benztropine when combined with either of two immunosuppressive drugs approved for the treatment of multiple sclerosis, interferon-β

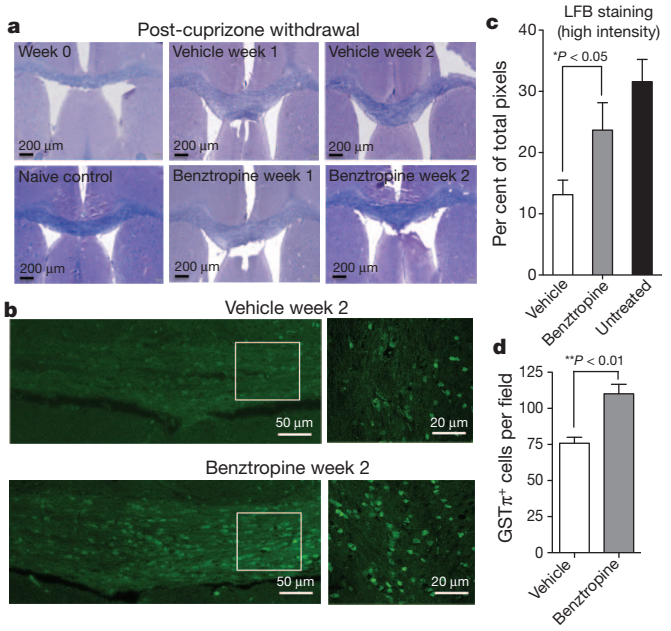

Figure 4 | Benztropine treatment enhances remyelination in the cuprizone model. **a**, Sections from the corpus callosum region of brains isolated from either benztropine- or vehicle-treated mice stained with Luxol fast blue. **b**, Quantification of Luxol fast blue (LFB) staining ($n = 6$ images each from 4 mice per group, mean and s.d., $^*P < 0.05$, *t*-test). **c**, Confocal microscopy images of sections from the corpus callosum region of brains isolated from either benztropine- or vehicle-treated mice immunostained for GST-π. **d**, Quantification of GST-π^+ mature oligodendrocytes. ($n = 20$ images each from 4 mice per group, mean and standard deviation, $^{**}P < 0.01$, *t*-test).

and FTY720 (refs 47, 48). The former reduces T-cell proliferation and alters cytokine expression[49], whereas the latter is an S1P agonist that blocks T-cell trafficking[50]. Initially, all three drugs were dosed individually over a range of concentrations to determine suboptimal and maximal effective/tolerated doses in the EAE model (Extended Data Figs 4a and 10a, b). Addition of 2.5 mg per kg of benztropine (suboptimal dose) to reported therapeutic doses of FTY720 (1 mg per kg) (Extended Data Fig. 10c) or interferon-β (10,000 U per mouse) (Extended Data Fig. 10d) resulted in decreased clinical severity comparable to, or greater than, either FTY720 or interferon-β alone. Furthermore, the combination of a suboptimal dose of benztropine (2.5 mg per kg) with a suboptimal dose of FTY720 (0.1 mg per kg) resulted in a significant decrease in clinical severity (Extended Data Fig. 10e) comparable to the clinical efficacy observed when FTY720 was given alone at the reported therapeutically effective dose of 1 mg per kg (Extended Data Fig. 10f). Addition of benztropine to FTY720 does not result in a decrease in immune cell infiltration compared to FTY720 treatment alone (Extended Data Fig. 10g, h), and addition of FTY720 to benztropine does not result in an increase in the number of oligodendrocytes compared to benztropine treatment alone (Extended Data Fig. 10i, j). This finding indicates that the observed benefit (Extended Data Fig. 10k) that results from this drug combination is derived from an additive effect that occurs when both immunological and remyelination mechanisms are targeted simultaneously. This observation may prove clinically relevant, because FTY720 treatment is associated with a dose-dependent bradycardia, which might be reduced by combination therapy with benztropine, and benztropine is associated with dose-dependent adverse neurological side effects.

Discussion

We have identified a centrally acting drug that, when administered in a clinically relevant model of multiple sclerosis, significantly decreases disease severity by directly stimulating the differentiation of a progenitor cell population leading to enhanced remyelination and functional recovery. Pharmacological data clearly indicates that the mechanism of action of benztropine is dependent on muscarinic receptor antagonism, but not any of its other known biological activities. However, based on the lack of activity of some of the anti-muscarinics tested, we cannot rule out the possibility that an additional unidentified target may exist that is common to all of the active anti-muscarinics identified. Further, although experimental evidence clearly indicates that benztropine induces OPC differentiation and remyelination *in vitro* and *in vivo*, it is possible that the therapeutic effect observed in the EAE model could also result in part from a protective effect derived from increased glial cell density. Inclusion of benztropine in EAE treatment regimens involving existing approved immunosuppressive drugs results in enhanced functional recovery and, in the case of FTY720, significantly decreases the dosages of both drugs that are required to achieve equivalent efficacy. Successful translation of these findings to multiple sclerosis patient populations will require further preclinical and clinical evaluation, as benztropine and other anti-muscarinics have significant dose-dependent neurological and psychiatric side effects. To our knowledge, these results provide the first *in vivo* evidence supporting the notion that benefit can be achieved by treating multiple-sclerosis-like symptoms using the combination of an immunosuppressive drug with a remyelination enhancer and may have a significant effect on the development of new and more effective therapies for the treatment of multiple sclerosis. Finally, we are evaluating other hits from our screen to identify compounds that induce remyelination by mechanisms distinct from that of benztropine.

METHODS SUMMARY

Cell culture and high-throughput screening. Primary rat optic nerve-derived OPCs were screened in 384-well format (1.5 µM compound) using basal differentiation conditions. Following immunostaining using an MBP-specific antibody, plates were imaged and analysed using Opera (Perkin Elmer) or Cell Insight (Thermo) high content imaging systems.

***In vivo* animal models.** The PLP-induced EAE model was performed and scored using 8-week-old female SJL/J mice as described[37]. Mice received daily i.p. injections with vehicle or drug using either prophylactic or therapeutic regimens. For the cuprizone model, C57BL/6 mice were fed 0.2% w/w cuprizone with chow for 7 weeks and thereafter with normal chow, at which point benztropine (10 mg per kg) or saline was injected daily (i.p.) starting for 5 weeks. Spinal cords were isolated and histological analysis was performed at weeks 0–5 following cuprizone withdrawal.

Online Content Any additional Methods, Extended Data display items and Source Data are available in the online version of the paper; references unique to these sections appear only in the online paper.

Received 4 January; accepted 10 September 2013.
Published online 9 October 2013.

1. Franklin, R. J. & Ffrench-Constant, C. Remyelination in the CNS: from biology to therapy. *Nature Rev. Neurosci.* **9,** 839–855 (2008).
2. Franklin, R. J. Why does remyelination fail in multiple sclerosis? *Nature Rev. Neurosci.* **3,** 705–714 (2002).
3. Nunes, M. C. *et al.* Identification and isolation of multipotential neural progenitor cells from the subcortical white matter of the adult human brain. *Nature Med.* **9,** 439–447 (2003).
4. Belachew, S. *et al.* Postnatal NG2 proteoglycan-expressing progenitor cells are intrinsically multipotent and generate functional neurons. *J. Cell Biol.* **161,** 169–186 (2003).
5. Huang, J. K. *et al.* Retinoid X receptor gamma signaling accelerates CNS remyelination. *Nature Neurosci.* **14,** 45–53 (2011).
6. Gensert, J. M. & Goldman, J. E. Endogenous progenitors remyelinate demyelinated axons in the adult CNS. *Neuron* **19,** 197–203 (1997).
7. Horner, P. J. *et al.* Proliferation and differentiation of progenitor cells throughout the intact adult rat spinal cord. *J. Neurosci.* **20,** 2218–2228 (2000).
8. Kremer, D., Aktas, O., Hartung, H. P. & Kury, P. The complex world of oligodendroglial differentiation inhibitors. *Ann. Neurol.* **69,** 602–618 (2011).
9. Patel, J. R. & Klein, R. S. Mediators of oligodendrocyte differentiation during remyelination. *FEBS Lett.* **585,** 3730–3737 (2011).
10. Chang, A., Tourtellotte, W. W., Rudick, R. & Trapp, B. D. Premyelinating oligodendrocytes in chronic lesions of multiple sclerosis. *N. Engl. J. Med.* **346,** 165–173 (2002).
11. Chari, D. M., Huang, W. L. & Blakemore, W. F. Dysfunctional oligodendrocyte progenitor cell (OPC) populations may inhibit repopulation of OPC depleted tissue. *J. Neurosci. Res.* **73,** 787–793 (2003).

12. Wolswijk, G. Chronic stage multiple sclerosis lesions contain a relatively quiescent population of oligodendrocyte precursor cells. *J. Neurosci.* **18,** 601–609 (1998).
13. Kuhlmann, T. *et al.* Differentiation block of oligodendroglial progenitor cells as a cause for remyelination failure in chronic multiple sclerosis. *Brain* **131,** 1749–1758 (2008).
14. Hart, I. K., Richardson, W. D., Bolsover, S. R. & Raff, M. C. PDGF and intracellular signaling in the timing of oligodendrocyte differentiation. *J. Cell Biol.* **109,** 3411–3417 (1989).
15. Billon, N., Tokumoto, Y., Forrest, D. & Raff, M. Role of thyroid hormone receptors in timing oligodendrocyte differentiation. *Dev. Biol.* **235,** 110–120 (2001).
16. Tokumoto, Y. M., Tang, D. G. & Raff, M. C. Two molecularly distinct intracellular pathways to oligodendrocyte differentiation: role of a p53 family protein. *EMBO J.* **20,** 5261–5268 (2001).
17. Fernandez, M. *et al.* Thyroid hormone administration enhances remyelination in chronic demyelinating inflammatory disease. *Proc. Natl Acad. Sci. USA* **101,** 16363–16368 (2004).
18. Calzà, L., Fernandez, M. & Giardino, L. Cellular approaches to central nervous system remyelination stimulation: thyroid hormone to promote myelin repair via endogenous stem and precursor cells. *J. Mol. Endocrinol.* **44,** 13–23 (2010).
19. Barres, B. A., Lazar, M. A. & Raff, M. C. A novel role for thyroid hormone, glucocorticoids and retinoic acid in timing oligodendrocyte development. *Development* **120,** 1097–1108 (1994).
20. Buckley, C. E. *et al.* Drug reprofiling using zebrafish identifies novel compounds with potential pro-myelination effects. *Neuropharmacology* **59,** 149–159 (2010).
21. Ibanez, C. *et al.* Steroids and the reversal of age-associated changes in myelination and remyelination. *Prog. Neurobiol.* **71,** 49–56 (2003).
22. Baer, A. S. *et al.* Myelin-mediated inhibition of oligodendrocyte precursor differentiation can be overcome by pharmacological modulation of Fyn-RhoA and protein kinase C signalling. *Brain* **132,** 465–481 (2009).
23. Joubert, L. *et al.* Chemical inducers and transcriptional markers of oligodendrocyte differentiation. *J. Neurosci. Res.* **88,** 2546–2557 (2010).
24. Gard, A. L. & Pfeiffer, S. E. Two proliferative stages of the oligodendrocyte lineage ($A2B5^+O4^-$ and $O4^+GalC^-$) under different mitogenic control. *Neuron* **5,** 615–625 (1990).
25. Pfeiffer, S. E., Warrington, A. E. & Bansal, R. The oligodendrocyte and its many cellular processes. *Trends Cell Biol.* **3,** 191–197 (1993).
26. Gaspard, N. *et al.* Generation of cortical neurons from mouse embryonic stem cells. *Nature Protocols* **4,** 1454–1463 (2009).
27. Barres, B. A. *et al.* Cell death and control of cell survival in the oligodendrocyte lineage. *Cell* **70,** 31–46 (1992).
28. Eshleman, A. J., Henningsen, R. A., Neve, K. A. & Janowsky, A. Release of dopamine via the human transporter. *Mol. Pharmacol.* **45,** 312–316 (1994).
29. McKearney, J. W. Stimulant actions of histamine H1 antagonists on operant behavior in the squirrel monkey. *Psychopharmacol.* **77,** 156–158 (1982).
30. Agoston, G. E. *et al.* Novel N-substituted 3α-[bis(4'-fluorophenyl)methoxy]tropane analogues: selective ligands for the dopamine transporter. *J. Med. Chem.* **40,** 4329–4339 (1997).
31. De Angelis, F., Bernardo, A., Magnaghi, V., Minghetti, L. & Tata, A. M. Muscarinic receptor subtypes as potential targets to modulate oligodendrocyte progenitor survival, proliferation and differentiation. *Dev. Neurobiol.* **72,** 713–728 (2012).
32. Stidworthy, M. F. *et al.* Notch1 and Jagged1 are expressed after CNS demyelination, but are not a major rate-determining factor during remyelination. *Brain* **127,** 1928–1941 (2004).
33. Taveggia, C., Feltri, M. L. & Wrabetz, L. Signals to promote myelin formation and repair. *Nature Rev. Neurol.* **6,** 276–287 (2010).
34. Ragheb, F. *et al.* Pharmacological and functional characterization of muscarinic receptor subtypes in developing oligodendrocytes. *J. Neurochem.* **77,** 1396–1406 (2001).
35. Felder, C. C. Muscarinic acetylcholine receptors: signal transduction through multiple effectors. *FASEB J.* **9,** 619–625 (1995).
36. Owens, T. & Sriram, S. The immunology of multiple sclerosis and its animal model, experimental allergic encephalomyelitis. *Neurol. Clin.* **13,** 51–73 (1995).
37. Lawson, B. R. *et al.* Inhibition of transmethylation down-regulates CD4 T cell activation and curtails development of autoimmunity in a model system. *J. Immunol.* **178,** 5366–5374 (2007).
38. Mix, E., Meyer-Rienecker, H. & Zettl, U. K. Animal models of multiple sclerosis for the development and validation of novel therapies—potential and limitations. *J. Neurol.* **255** (Suppl 6), 7–14 (2008).
39. Steinman, L. & Zamvil, S. S. Virtues and pitfalls of EAE for the development of therapies for multiple sclerosis. *Trends Immunol.* **26,** 565–571 (2005).
40. Aharoni, R. *et al.* Distinct pathological patterns in relapsing-remitting and chronic models of experimental autoimmune enchephalomyelitis and the neuroprotective effect of glatiramer acetate. *J. Autoimmun.* **37,** 228–241 (2011).
41. Liu, L. *et al.* Myelin repair is accelerated by inactivating CXCR2 on nonhematopoietic cells. *J. Neurosci.* **30,** 9074–9083 (2010).
42. Mi, S. *et al.* LINGO-1 antagonist promotes spinal cord remyelination and axonal integrity in MOG-induced experimental autoimmune encephalomyelitis. *Nature Med.* **13,** 1228–1233 (2007).
43. Kawashima, K. & Fujii, T. Basic and clinical aspects of non-neuronal acetylcholine: overview of non-neuronal cholinergic systems and their biological significance. *J. Pharmacol. Sci.* **106,** 167–173 (2008).
44. Stern, J. N. *et al.* Promoting tolerance to proteolipid protein-induced experimental autoimmune encephalomyelitis through targeting dendritic cells. *Proc. Natl Acad. Sci. USA* **107,** 17280–17285 (2010).
45. Steelman, A. J., Thompson, J. P. & Li, J. Demyelination and remyelination in anatomically distinct regions of the corpus callosum following cuprizone intoxication. *Neurosci. Res.* **72,** 32–42 (2012).
46. Matsushima, G. K. & Morell, P. The neurotoxicant, cuprizone, as a model to study demyelination and remyelination in the central nervous system. *Brain Pathol.* **11,** 107–116 (2001).
47. Kappos, L. *et al.* Oral fingolimod (FTY720) for relapsing multiple sclerosis. *N. Engl. J. Med.* **355,** 1124–1140 (2006).
48. Durelli, L. *et al.* Every-other-day interferon beta-1b versus once-weekly interferon beta-1a for multiple sclerosis: results of a 2-year prospective randomised multicentre study (INCOMIN). *Lancet* **359,** 1453–1460 (2002).
49. Noronha, A., Toscas, A. & Jensen, M. A. Interferon β decreases T cell activation and interferon γ production in multiple sclerosis. *J. Neuroimmunol.* **46,** 145–153 (1993).
50. Brinkmann, V. *et al.* The immune modulator FTY720 targets sphingosine 1-phosphate receptors. *J. Biol. Chem.* **277,** 21453–21457 (2002).

Supplementary Information is available in the online version of the paper.

Acknowledgements This work was supported by the Skaggs Institute for Chemical Biology and the California Institute for Regenerative Medicine grant TR3-05617 (to P.G.S), the California Institute for Regenerative Medicine (TG2-01165) and National Science Foundation pre-doctoral fellowships (to V.A.D and C.A.L, respectively). We are grateful to T. Hasnat, M. Chadwell, W. Kiosses and M. Wood for technical support. This is manuscript number 21786 of The Scripps Research Institute.

Author Contributions L.L.L., P.G.S., C.A.L. and V.A.D. initiated the project and developed strategy. V.A.D., V.T., C.C.G., B.K., H.J.K., K.P., J.G.S. and I.A. performed the experiments. L.L.L., P.G.S. and V.A.D.wrote the manuscript. B.R.L., C.A.L., A.N.T., F.H.G. and T.K. contributed essential ideas and comments.

Author Information Reprints and permissions information is available at www.nature.com/reprints. The authors declare no competing financial interests. Readers are welcome to comment on the online version of the paper. Correspondence and requests for materials should be addressed to B.L. (blawson@scripps.edu), P.G.S. (schultz@scripps.edu) or L.L.L. (llairson@scripps.edu).

METHODS

Statistical methods and experimental design. High-throughput screening was performed at a single concentration (1.5 μM) and primary hits were reconfirmed in triplicate. In all *in vivo* animal studies, we calculated that we required 8–12 mice per group in order to have 80% power of detecting approximately a 30% change, assuming a standard deviation of 30% at a significance level of $\alpha = 0.05$. It has been our experience that this is sufficient to detect clinically and statistically significant differences with repetitive studies. As per standard scoring methods for EAE, mice found moribund or dead were scored as 5 for the remainder of the study. For therapeutic dosing, just before drug treatment, mice were randomized, based on clinical severity such that each treatment group had equivalent mean clinical EAE scores. Mice were scored non-blinded. For all experiments, assuming normal distribution, two-sided *t*-tests were used to evaluate comparisons between 2 groups and ANOVA was used when >2 groups were compared. For the quantitative analysis of *in vitro* myelination, ANOVA with Bonferroni correction was used. Where possible, data are represented as mean ± s.e.m., otherwise data are represented as mean ± s.d., as indicated in the figure legends.

Cell culture. Rat primary optic nerve OPCs were isolated by panning[27,51] (>99% $A2B5^+$) and cultured in poly-D-lysine (10 μg ml^{-1})-coated flasks in OPC proliferation media (Neurobasal Media, Invitrogen) supplemented with B27-without vitamin A (Invitrogen), non-essential amino acids, L-glutamine and PDGF-AA (30 ng ml^{-1}; Peprotech)) at 37 °C with 5% CO_2. OPCs were used between passage 10 and 15 and were never allowed to reach confluence to maintain a naive state. For differentiation, OPCs were plated in differentiation media (Neurobasal Media (Invitrogen) supplemented with B27-without vitamin A (Invitrogen), non-essential amino acids, L-glutamine and PDGF-AA (2 ng ml^{-1}; Peprotech)).

Mouse cortical neural cell mixture was prepared from E18.5 brain using the Papain dissociation system, according to the supplier's instructions kit (Worthington Biochemical). Then, both oligodendrocytes and OPCs were depleted from the mixture by sequential immunopanning as described previously[27,52]. The cells were then cultured on poly-D-lysine-coated 8-well chamber slide (Nunc) as described previously[53]. Mouse neural stem cells (Invitrogen) were cultured in OPC medium as described previously[54]. Induced mouse OPCs (5,000 cells per well) were cultured with benztropine on the cortex-derived culture for 7 days. Cells were immunolabelled as described previously[51].

High-throughput screening and imaging. OPCs were plated at a density of 1,000 cells per well on poly-D-lysine (10 μg ml^{-1}) coated 384-well plates (Greiner) in differentiation media. Compounds were added at a final concentration of 1.5 μM within 12 h after plating the cells and incubated at 37 °C with 5% CO_2 for 6 days. Cells were then fixed for 20 min with 4% formaldehyde solution and stained with mouse anti-rat MBP antibody (Millipore) in 3% BSA, 0.3% Triton X-100 with overnight incubation at 4 °C. The cells were washed and incubated with secondary antibody (goat anti-mouse Alexa Fluor488) and DAPI (Invitrogen) for 1 h at room temperature. The cells were washed and plates were sealed and imaged using an Opera confocal imaging reader (Perkin Elmer) or a Cellomics Cell Insight imaging reader (Thermo). An air ×10 lens was used to capture 9 images per well at both wavelengths (488 and 365 nm), representing different locations in a single well. For image analysis, DAPI-stained nuclei and MBP-positive cell bodies were detected using an algorithm that selects for positive cell bodies and nuclei within a range of fluorescent emission values and sizes as determined by fitting parameters to positive (thyroid hormone (T3), 1 μM) and negative controls (DMSO, 0.1%). Numerical results from the analysed images were later exported for analysis in Excel (Microsoft) and Spotfire (Tibco).

Data analysis. EC_{50} values were obtained by fitting the data using the sigmoidal dose–response curve-fitting function (Prism; GraphPad Software). Eight or twelve different concentrations and three data points per concentration were usually used for curve fitting. Experiments were repeated 2 or more times.

Compounds. Hit compounds were purchased as powders and dissolved in DMSO for *in vitro* studies or saline for *in vivo* studies. Benztropine mesylate (MP Biomedicals), mycophenolate mofetil (Selleck Chemicals), FTY720 (Cayman Chemical), carbachol (EMD Chemicals), haloperidol (Sigma), quinpirole (Sigma), interferon-β, ipratropium (Sigma), oxybutynin (Sigma), histamine (Acros Organics), scopolamine (Sigma), atropine (Sigma), histamine trifluoromethyl toluidide (HTMT; Tocris Bioscience).

***In vitro* myelination.** Mouse embryonic stem cells (ES cells) were differentiated into neurons using a previously published protocol[26]. Neurons were allowed to mature and extend axons for about one week before plating rat primary OPCs. Cells were treated with either DMSO or 1 μM T3 or 1 μM benztropine for two weeks and myelination under different conditions was quantified. For quantification, co-cultures were fixed for 15 min in 4% PFA and stained with TUJ1 (rabbit; Covance) and MBP (mouse; Millipore) antibodies. A total of 10 randomly selected regions on 2 plates per experiment were imaged. Images were imported to Imaris (Bitplane), and axon, oligodendrocyte processes were identified. Rendered channels of the processes were exported as TIFF files to be analysed further using a custom script in MATLAB (Mathworks). Myelination was identified as regions of co-localization between MBP positive oligodendrocyte processes and TUJ1 positive neurites. Cell bodies were eliminated from the analysis to reduce the error due to non-specific overlap of MBP and TUJ1 staining.

Immunocytochemistry and antibodies. Immunostaining of cells was performed using standard protocols. Primary antibodies and dilutions are provided in Supplementary Table 4. Secondary antibodies were Alexa Fluor488 or Alexa Fluor647 conjugated anti-rabbit or anti-mouse (1:500; Invitrogen). Nuclei were counterstained with DAPI. Cells were imaged using a Nikon confocal microscope with a ×10 air lens.

Western blot analysis. OPCs were plated in basal differentiation medium and treated for 6 days with benztropine (1.5 μM), T3 (1 μM) or DMSO. Cells were collected by scraping, pelleted and washed with ice-cold phosphate buffered saline (PBS) before lysis with PBS containing protease inhibitors (Roche), phosphatase inhibitors (Sigma), Triton X-100 and EDTA. Following incubation on ice for 20 min, lysed cells were centrifuged (16,000*g*, 15 min at 4 °C). Total protein was quantified using a NanoDrop and equal amounts of protein from each sample was denatured by boiling with 4× SDS sample buffer (Invitrogen) containing β-mercaptoethanol (5%). Proteins were electrophoresed using 4–20% SDS–PAGE gels (BioRad) and transferred on to a nitrocellulose membrane (BioRad). The membrane was blocked with 5% non-fat dry milk in TRIS buffered saline with Tween-20 (0.2%) and reacted with appropriate antibodies. Blots were incubated with HRP-conjugated secondary antibodies and visualized using film and Super Signal West peroxide solution (Pierce).

Semi-quantitative RT–PCR analysis. Total RNA from different samples was isolated and purified using the RNeasy mini kit (Qiagen) with on-column DNase digestion according to the manufacturer's protocol. Single-stranded cDNA was synthesized from 3 μg of total RNA with the SuperScript III First-Strand Synthesis System for RT–PCR using oligo$(dT)_{20}$ primers (Invitrogen). PCRs were performed using the Phusion High Fidelity polymerase and gene-specific primers (Supplementary Table 5). Cycle parameters for all genes were 30 s at 94 °C, 60 s at 57 °C and 60 s at 72 °C for 25 cycles.

Quantitative RT–PCR. For expression analysis of MBP, MOG, cyclin D1, cyclin D2, *c-Fos* and *c-Jun*, RNA was isolated and reverse-transcribed to complementary DNA (cDNA) as previously described. cDNA was used for qRT–PCR with gene-specific Taqman probes labelled with FAM (Applied Biosystems). qRT–PCR was performed using the ABI 7900HT instrument (Applied Biosystems) with standard parameters. The amount of cDNA was optimized so that amplification of both control genes and the cDNAs of interest were in the exponential phase. Transcripts were quantitated by comparative C_t method and normalized to endogenous controls, β-actin and GAPDH.

For expression analysis of other genes, RNA was isolated and reverse-transcribed to cDNA as previously described. cDNA was used for SBYR-green based qRT–PCR using gene-specific primers (Supplementary Table 5). Transcripts were quantitated by comparative C_t method and normalized to endogenous controls, 18S, β-actin and GAPDH.

Cyclic AMP HTRF assay. OPCs were plated at a density of 8,000 cells per well onto a 384-well plate and incubated at 37 °C overnight. The assay was performed using the HRTF cAMP dynamic 2 kit (CisBio Bioassays) per the manufacturer's protocol. IBMX (1 μM final concentration) was added as a cAMP stabilizer. Data acquisition was performed in the time-resolved fluorescence resonance energy transfer (FRET) mode on Envision (PerkinElmer). The ratio between the acceptor fluorescence signal ($A_{665\,nm}$) and donor fluorescence signal ($A_{620\,nm}$) $\times 10^4$, representing the FRET between the conjugated cAMP and the anti-cAMP antibody, was calculated and plotted on the *y* axis. The ratio is inversely proportional to the endogenous cAMP levels in the sample.

Calcium influx assay. Effect of compound treatment on the release of Ca^{2+} ions from the ER was measured using the FLIPR Tetra system (Molecular Devices). Briefly, cells were treated with carbachol as an M1/M3 agonist and the compounds were assayed for M1/M3 receptor antagonism using a Ca^{2+} sensitive Fluo-3AM dye.

EAE model. SJL/J (8-week-old female) mice were purchased from The Jackson Laboratory. Mice were immunized subcutaneously with murine proteolipid peptide ($PLP_{139\text{-}151}$; Peptides International) mixed 1:1 with supplemented complete Freund's adjuvant (CFA, Fisher) followed by *Bordetella pertussis* toxin (200 μg per mouse, Sigma) on day 0 and day 2 as described[37]. Clinical EAE was graded on a scale of 1–5 by established standard criteria as follows: score 0, no observable disease; score 1, limp tail; score 2, limp tail and partial limb weakness; score 3, one hind limb paralyzed; score 4, both hind limbs paralyzed; score 5, moribund/dead. Mice received daily i.p. injections with compounds dissolved in saline. Dosing was commenced either on the day of PLP injections defined as prophylactic regimen or at the first appearance of EAE symptoms defined as therapeutic regimen and continued until day 30.

Immunohistochemistry and antibodies. Spinal cords were isolated from mice using standard protocols, fixed in Formalin-Zinc overnight followed by incubation in 30% sucrose at 4 °C overnight. Spinal cords were cross-sectioned into 8 pieces and embedded in Tissue-Tek OCT (Electron Microscopy Sciences). Thin sections were cut using a Leica cryostat and stained for myelin and infiltrating cells using Luxol fast blue, PAS, haematoxylin and eosin using standard protocols. For OPC and oligodendrocyte staining, sections were treated with Cirtisolve (Fisher) antigen retrieval solution, followed by incubation with primary antibodies (Supplementary Table 3). Secondary antibodies were Alexa Fluor488 or Alexa Fluor647-conjugated anti-rabbit or anti-mouse (1:500; Invitrogen). Nuclei were counterstained with DAPI. Cells were imaged using a Zeiss confocal microscope. Quantitative image analysis was performed using ImageJ (NIH) and ImagePro (Media Cybernetics). Numerical results from the analysed images were exported for analysis in Excel (Microsoft).

Brains from cuprizone-treated mice were isolated using standard protocols, fixed in formalin-zinc overnight, and embedded in paraffin. Sections were deparaffinized using a standard protocol and stained with Luxol fast blue (LFB) and haematoxylin and eosin as previously described. Slides were scanned using a Leica scanner. Images from at least 6 sections were collected and quantitative image analysis was performed using ImageJ (National Institutes of Health) and ImagePro (Media Cybernetics). Numerical results from the analysed images were exported for analysis in Excel (Microsoft).

Electron microscopy. Mice were exsanguinated with 0.9% saline followed by perfusion fixation with 4% paraformaldehyde, 1.5% glutaraldehyde and 1 mM $CaCl_2$ in 0.1 M cacodylate buffer and the spinal cords were exposed and fixed *in situ* overnight. Following complete removal, immersion fixation continued overnight at 4 °C in cacodylate buffered 2.5% glutaraldehyde with 1 mM $CaCl_2$ and then sliced into individual blocks. The tissues were then buffer washed, fixed in 1% osmium tetroxide and subsequently dehydrated in graded ethanol series, transitioned in propylene oxide and embedded in EMbed 812 / Araldite (Electron Microscopy Sciences). Thick sections (1.5 μm) were cut, mounted on glass slides and stained in toluidine blue for general assessment in the light microscope. Subsequently, 70-nm thin sections were cut with a diamond knife (Diatome), mounted on copper slot grids coated with parlodion and stained with uranyl acetate and lead citrate for examination on a Philips CM100 electron microscope (FEI) at 80 kV. Images were documented using a Megaview III CCD camera (Olympus Soft Imaging Solutions). Images were analysed in Image-Pro for *g*-ratio measurements by manually drawing lines across 2 perpendicular diameters each for axons and axons plus myelin. Lengths of the lines (in pixels) as generated by Image-Pro were averaged across the 2 perpendicular measurements and converted to micrometres (μm) using the image scale bars. *g*-ratio is defined as the ratio of the diameter of a given axon and the diameter of the axon plus myelin unit. Approximately 1,000 axons and axon plus myelin units were measured for each treatment group.

***In vitro* T-cell assay.** Spleens were isolated from SJL/J, teased apart to single cell suspensions, red blood cells were lysed and remaining cells were isolated by centrifugation, resuspended in complete media and counted. The cells were then plated with soluble anti-CD28 (5 μg ml^{-1}) at 2×10^5cells per well on plates pre-coated with anti-CD3 (10 μg ml^{-1}). Compounds dissolved in dimethylsulphoxide (DMSO) (<0.1%) were added at 4 different dilutions (5 mM, 500 μM, 50 μM, 5 μM) and incubated at 37 °C, 5% CO_2 for 24, 48, 72 and 96 h. Cells were analysed by flow cytometry for CFSE dilution and CD25 and CD69 expression. Cells were labelled with CFSE (3 μM) in PBS supplemented with bovine serum albumin (BSA, 0.1%). Labelling was performed in the dark at 37 °C for 10 min with occasional mixing. Labelling was stopped by addition of 5 volumes of ice-cold PBS (0.1% BSA). Labelled cells were cultured for two days and analysed on a LSR II flow cytometer (Becton Dickinson). The data was analysed using the FloJo software (Tree Star).

***In vivo* T-cell assay.** SJL/J (8-week-old female) mice were injected with PLP and *Pertussis* toxin to induce EAE as described in the previous section. On the same day, a prophylactic dosing regimen of compounds dissolved in saline was commenced by i.p. injections. The mice were scored and dosed daily. Mice usually developed symptoms of EAE by day 9, with the peak of symptoms appearing around day 14. Mice were sacrificed on day 14 and spleens were removed. Blood was collected for sera. Spleens were teased apart to single cell suspensions, red blood cells were lysed and splenocytes were isolated by centrifugation. Cells were resuspended in complete medium defined as Dulbecco's modified eagle medium (Gibco) supplemented with 10% fetal bovine serum (Gibco) and counted. Cells were then plated at 2×10^5 cells per well on a 96-well plate and treated with either 20 μg ml^{-1} PLP peptide or 10 ng ml^{-1} phorbol myristate acetate (PMA) and 300 ng ml^{-1} ionomycin for 48 h to stimulate cytokine production. Cytokine secretion was blocked during the last 5 h by treatment with monensin. Supernatants were collected for ELISAs of IL-2, IFN-γ, IL-10 and TNF-α. Cells were stained for flow cytometry using antibodies against CD4, CD8, B220 and CD44. Cells were also stained for intracellular cytokines such as IL-2, IFN-γ, IL-10 and TNF-α along with anti-CD4. Flow cytometry analysis was performed on a LSR II flow cytometer (Becton Dickinson) and the data was analysed using the FloJo software (Tree Star).

***In vivo* assays for T-cell-dependent B-cell responses.** SJL/J mice were injected i.p. with TNP-KLH (Biosearch Technology; 25 μg per mouse in complete Freund's adjuvant). Benztropine (10 mg per kg) or vehicle was injected i.p. daily for 21 days. Sera were collected on day 0, 7, 14 and 21. The collected sera was analysed by ELISA for anti-TNP IgG levels.

Bone marrow-derived macrophages and M1/M2 polarization. Bone marrow-derived macrophage (BMM) cultures were generated from adult SJL/J mice. Briefly, femurs and tibias were collected bilaterally and marrow cores were flushed using syringes filled with DMEM medium supplemented by with 1% penicillin/streptomycin, 1% HEPES, 1% sodium pyruvate, 0.1% β-mercaptoethanol and 10% FBS (complete DMEM) (Gibco). Cells suspension were filtered through a 0.2 μm cell strainer, counted, plated in complete DMEM supplemented with 5% of horse serum and 20% supernatant from macrophage colony stimulating factor secreting L929 (sL929) cells. The sL929 drives bone marrow cells towards a macrophage phenotype (10 days). Non-adherent cells were removed at day 4. At collection (day 10), 90 ± 0.7% of cells were macrophages (assessed by F4/80 immunostaining). To promote differentiation into M1 or M2 macrophages, cells were treated with LPS (100 ng ml^{-1}; Sigma-Aldrich) plus IFNγ (20 ng ml^{-1}; Peprotech) or IL-4 plus IL-13 (20 ng ml^{-1}; Peprotech), respectively, for 16 h, in the presence or absence of benztropine (5 μM). After M1 or M2 polarization, some cells (cultured without benztropine) were saved and treated once again, as described above. The viability of M1/M2 macrophages was analysed in every experiment by flow cytometry of DAPI-stained cells (Invitrogen). Supernatants and cells were subsequently collected for cytokine (TNF-α) and phenotypic analysis, respectively. M1 and M2 polarization was assessed using the following fluorochrome-labelled antibodies: anti-F4/80, rat anti-mouse mannose receptor (CD206), rat anti-mouse CD86, rat anti-mouse CD80 and anti-mouse I-A/I-E antibodies (BioLegend).

Isolation of spleen and leukocyte isolation from spinal cords. EAE mice were euthanized, spleens were isolated from the mice as per standard protocols and crushed by mechanical disruption using a tissue homogenizer. Spinal cords were isolated from the mice, treated with collagenase and ground to a single cell suspension. Suspensions from 2 spinal cords from mice with similar clinical severity scores were combined and centrifuged through gradients of 30% and 70% Percoll to isolate infiltrating leukocytes. Total RNA was isolated and used for gene expression analysis as previously described.

Adoptive transfer EAE. SJL/J donor mice were purchased from The Jackson Laboratories. Mice were immunized subcutaneously with murine proteolipid peptide ($PLP_{139\text{-}151}$; Peptides International) mixed 1:1 with supplemented complete Freund's adjuvant (CFA, Fisher). Mice were then either injected with saline or benztropine (10 mg per kg, daily, i.p.) for 7 days, and re-immunized with murine PLP emulsified 1:1 with incomplete Freund's adjuvant. Daily benztropine or vehicle injections were continued until day 10, when spleens were isolated, teased apart to single cell suspensions, red blood cells lysed and splenocytes isolated by centrifugation. Cells were resuspended in complete media (RPMI 1640 supplemented with 10% fetal bovine serum (FBS), 1.25% HEPES buffer, 1% sodium pyruvate, 1% penicillin-strepyomycin, 1% glutamine, 1% non-essential amino acids, 0.01% 2-mercaptoethanol (2-ME)) (Sigma-Aldrich) and counted. Splenocytes were analysed by flow cytometry to determine cell viability and percentage of $CD4^+$ T cells as described earlier. Splenocytes from vehicle-treated mice were further cultured *in vitro* in the presence of $PLP_{139\text{-}151}$ (30 μg ml^{-1}), interleukin 12 (IL-12) (10 ng ml^{-1}) and DMSO (<0.1%), whereas splenocytes from benztropine-treated donor mice were further cultured *in vitro* in the presence of $PLP_{139\text{-}151}$, interlukin 12 (IL-12) (10 ng ml^{-1}) and benztropine (5 μM) for 72 h at 37 °C. At the end of 72 h, cells were analysed by flow cytometry to determine cell viability and percentage of $CD4^+$ T cells as described earlier (~80% activated T cells after *in vitro* culture). Cells were then washed and resuspended in PBS (50 million cells ml^{-1}) and 200 μl of cell suspension was injected into 4 groups (according to the following table) of naive recipient SJL/J mice by intravenous injection followed by *Bordetella pertussis* toxin (i.p., 200 μg per mouse, Sigma) on day 0 and day 2. Clinical EAE was graded on a scale of 1–5 by established standard criteria as follows: score 0, no observable disease; score 1, limp tail; score 2, limp tail and partial limb weakness; score 3, one hind limb paralyzed; score 4, both hind limbs paralyzed; score 5, moribund/dead. Mice received daily i.p. injections of either saline or benztropine (10 mg per kg) according to Extended Data Fig. 8c, d.

Cuprizone model. C57BL/6 mice (8-week-old females) were purchased from the breeding colony at The Scripps Research Institute. Mice were fed 0.2% w/w cuprizone (bis-cyclohexanone oxaldihydrazone, Sigma-Aldrich) mixed into a ground standard rodent chow (Harlan). Cuprizone diet was maintained for 7 weeks; thereafter mice were put on a normal chow for another 5 weeks. Compounds were

dissolved in saline and daily i.p. injections were initiated at the withdrawal of the cuprizone diet. At different time points (0, 1, 2, 3, 4 and 5 weeks after cuprizone withdrawal), animals were euthanized. Brains were extracted, fixed in formalin-zinc, paraffin-embedded, sectioned and stained as described in the immunohistochemistry section.

Image analysis of brain sections. Using ImageJ (NIH), images were converted to a 256-shade grey scale. The 256 shades of grey were then divided into 5 bins of 50 shades each: 0–50, 50–100, 100–150, 150–200 and 200–256, with 0 being the pixel with darkest shade of grey and 256 being the pixel with the lightest shade of grey. Each bin was assigned an arbitrary colour: 0–50 (red), 50–100 (yellow), 100–150 (green), 150–200 (light blue) and 200–256 (dark blue). Based on the intensity of staining, each pixel was classified into one of the 5 bins using Image-Pro plus software. The number of objects in the corpus callosum region classified into each bin was counted. Data was exported to Excel (Microsoft) for analysis.

Animal use statement:. All experiments were performed in accordance with approved Institutional Animal Care and Use Committee (IACUC) protocols of The Scripps Research Institute or Hokkaido University Institute for Genetic Medicine.

51. Kondo, T. & Raff, M. The Id4 HLH protein and the timing of oligodendrocyte differentiation. *EMBO J.* **19,** 1998–2007 (2000).
52. Wang, S., Sdrulla, A., Johnson, J. E., Yokota, Y. & Barres, B. A. A role for the helix-loop-helix protein Id2 in the control of oligodendrocyte development. *Neuron* **29,** 603–614 (2001).
53. Pang, Y. *et al.* Neuron-oligodendrocyte myelination co-culture derived from embryonic rat spinal cord and cerebral cortex. *Brain Behav.* **2,** 53–67 (2012).
54. Izrael, M. *et al.* Human oligodendrocytes derived from embryonic stem cells: Effect of noggin on phenotypic differentiation *in vitro* and on myelination *in vivo*. *Mol. Cell. Neurosci.* **34,** 310–323 (2007).

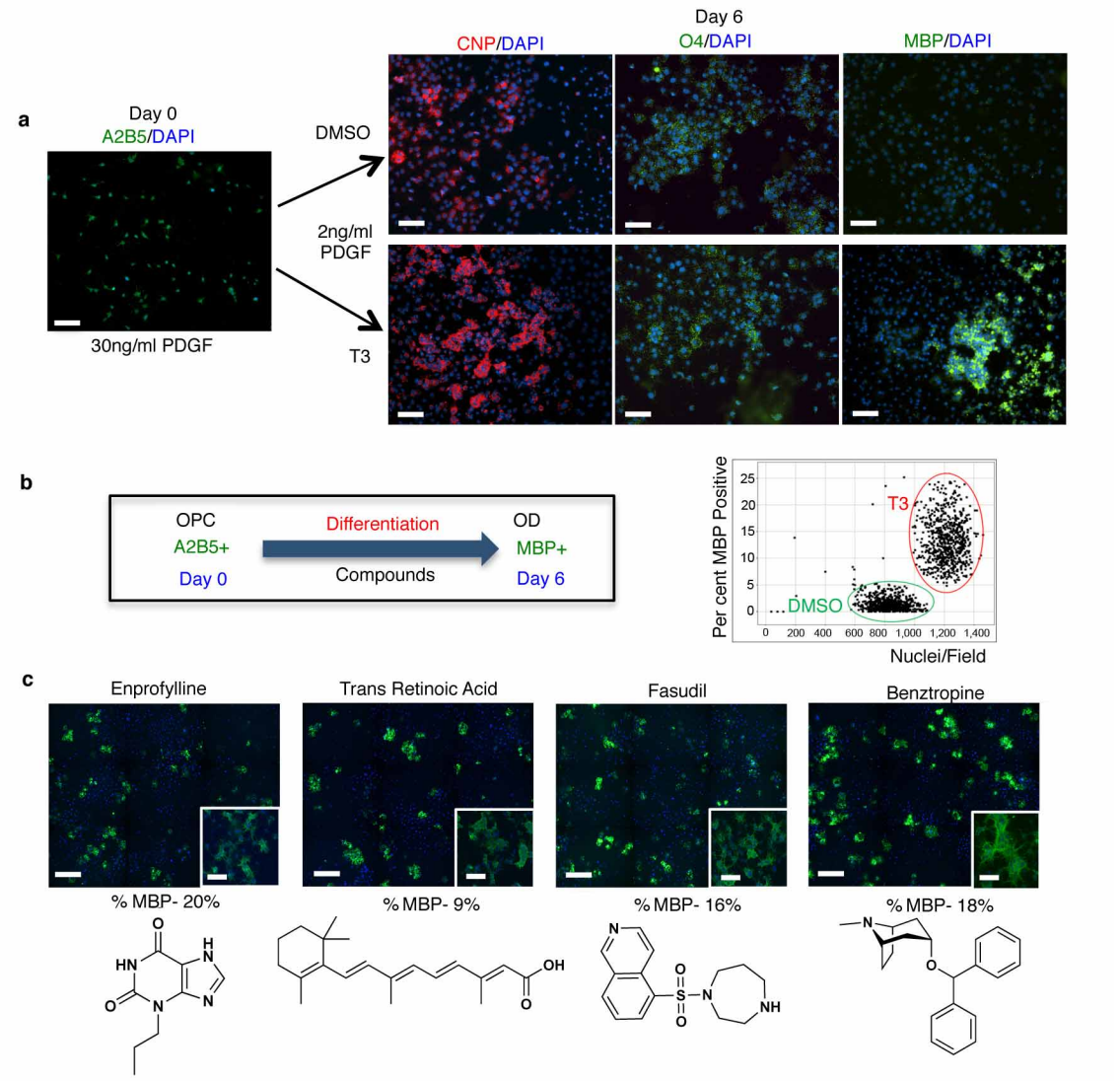

Extended Data Figure 1 | High-throughput screen to identify inducers of OPC differentiation. **a**, Rat primary OPCs in basal differentiation media treated with DMSO (<0.1%) or thyroid hormone (T3; 1 μM) for 6 days in culture, fixed and stained using antibodies for myelin basic protein (MBP), 2′,3′-cyclic-nucleotide 3′-phosphodiesterase (CNP) and oligodendrocyte marker O4. $A2B5^+$ OPCs differentiated into immature oligodendrocytes that express CNP and O4, but not MBP, upon reduction of PDGF-AA. T3 added as a positive control induced differentiation to mature cells that express MBP. Scale bars, 100 μm. **b**, Schematic representation of the high-throughput screening platform used to identify inducers of OPC differentiation. **c**, Inducers of OPC differentiation identified as hits from a screen of known biologically active compounds. Scale bars, 100 μm; inset, 40 μm.

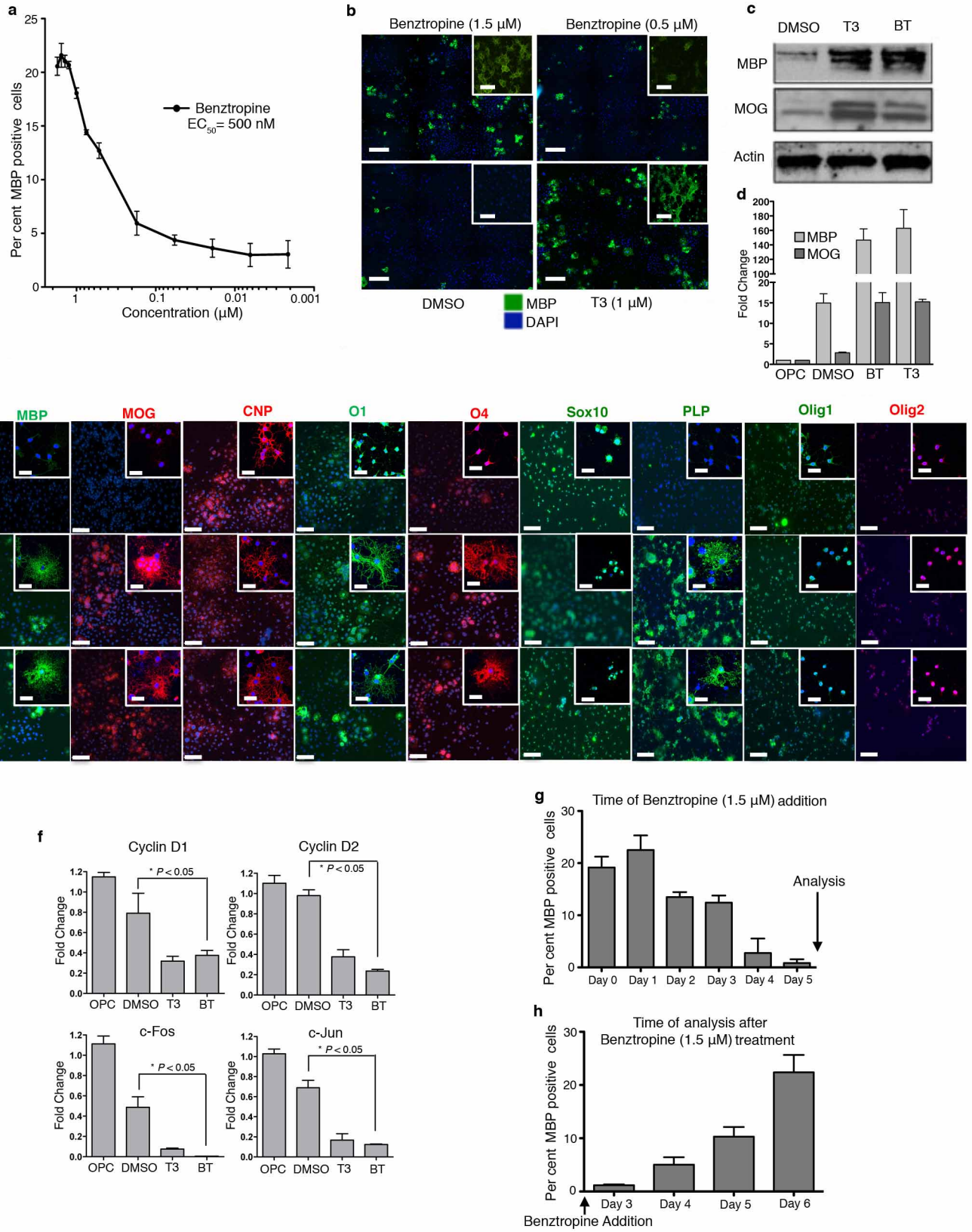

Extended Data Figure 2 | Benztropine induces dose-dependent OPC differentiation *in vitro* to mature oligodendrocytes. **a**, Dose response assay used to confirm primary screening activity of benztropine and determine potency (EC_{50}). OPCs were treated with benztropine and immunostained using antibodies for MBP ($n = 3$, mean and s.d.). **b**, Images showing dose-dependent induction of OPC differentiation after treatment with benztropine. (Scale bars, 100 μm; inset, 40 μm). OPCs in basal differentiation media treated with DMSO (<0.1%), T3 (1 μM) or benztropine (1.5 μM) for 6 days and analysed for MBP and MOG expression by western blot (**c**) and by qRT–PCR (**d**) ($n = 3$, mean and s.d.). **e**, OPCs were plated in differentiation medium and treated with DMSO (<0.1%), benztropine (1.5 μM) or T3 (1 μM) for 6 days. Cells were fixed and immunostained for myelin basic protein (MBP), myelin oligodendroglial glycoprotein (MOG), CNP, oligodendrocyte marker O1, oligodendrocyte marker O4, glial marker SOX10, proteolipid peptide (PLP), OLIG1 and OLIG2. Representative images showing expression of mature oligodendrocyte markers in benztropine- and T3-treated cells, but not DMSO-treated cells. Scale bars, 100 μm; inset, 40 μm. **f**, Expression of cell cycle genes by qRT–PCR. ($n = 3$, mean and s.d., $^*P < 0.05$, *t*-test). **g**, OPCs plated in basal differentiation medium and treated with benztropine (1.5 μM) on various days (0, 1, 2, 3, 4 and 5), fixed on day 6 and immunostained for MBP ($n = 3$, mean and s.d.). **h**, OPCs plated in basal differentiation medium, treated with benztropine (1.5 μM) on the same day, fixed on various days (3, 4, 5 and 6) following compound treatment and immunostained for MBP ($n = 3$, mean and s.d.).

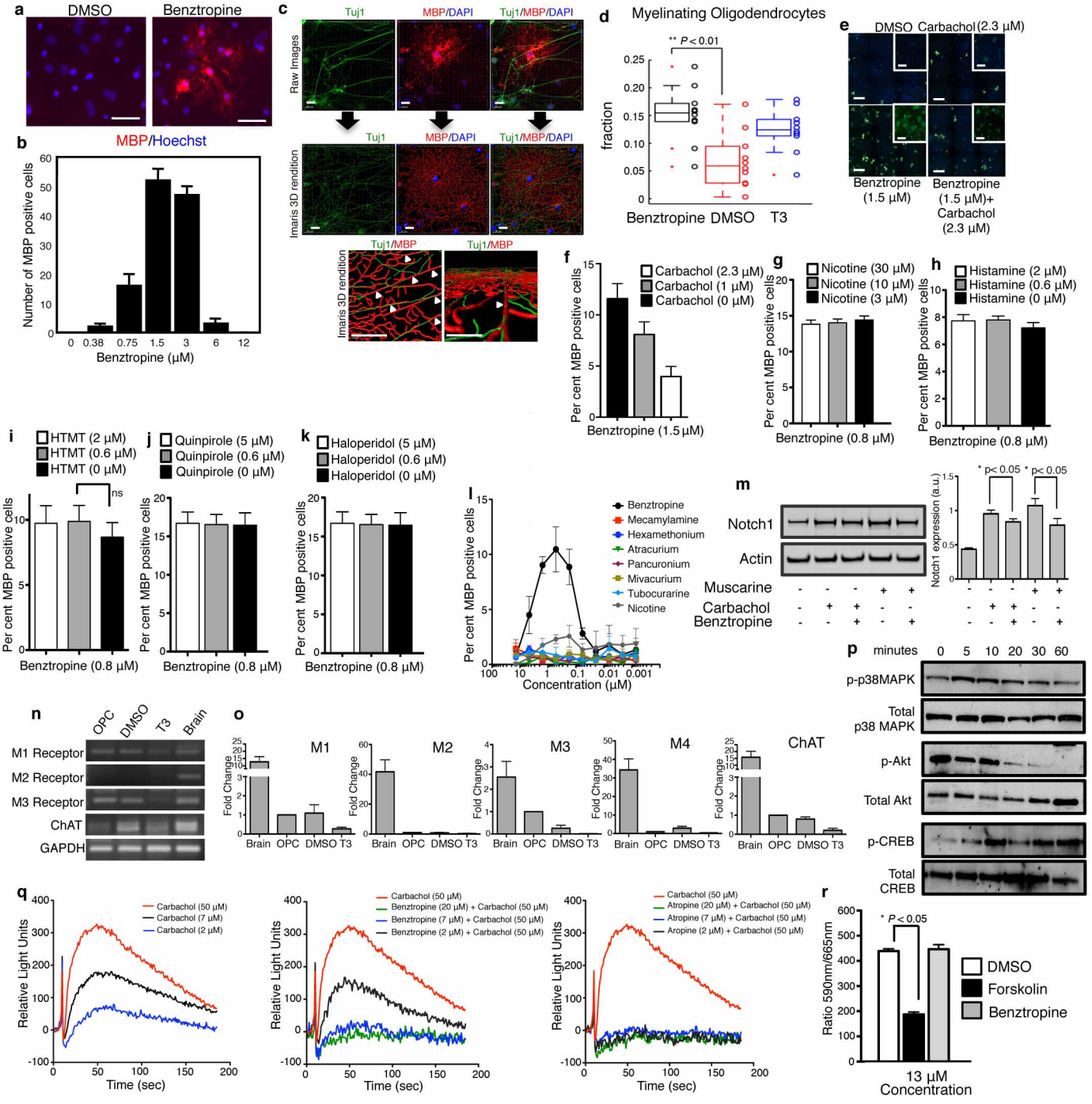

Extended Data Figure 3 | Benztropine induces OPC differentiation and *in vitro* myelination through M1/M3 muscarinic receptor antagonism and has no effect on histamine or nicotinic signalling. **a**, Mouse OPCs co-cultured with mouse cortex-derived cells in the presence of DMSO or benztropine and immunostained for MBP (red) and nuclei with Hoechst 33342 (blue). Scale bars, 100 μm. **b**, Quantification of MBP staining of mouse OPCs treated with DMSO or benztropine. **c**, Analysis of myelination in OPCs with neurons co-culture. Arrowheads point to regions of myelination. Scale bars, 20 μm. **d**, Quantification of fraction of myelinating oligodendrocytes in OPCs with neurons co-cultures ($n = 10$, mean and s.e.m., $^{**}P < 0.01$, ANOVA with Bonferroni correction). OPCs co-treated with benztropine (1.5 μM) and carbachol (2.3 μM) for 6 days and stained for MBP (green) (Scale bars, 100 μm; inset, 40 μm). **e**, Antagonism of benztropine-induced OPC differentiation by muscarinic agonist carbachol. **f**, Quantification of MBP staining of OPCs co-treated with benztropine (1.5 μM) and muscarinic receptor agonist carbachol for 6 days under basal differentiation conditions ($n = 3$, mean and s.d.). **g**–**k**, OPCs plated co-treated with benztropine (0.8 μM) and either nicotine (**g**), histamine (**h**), histamine receptor agonist histamine trifluoromethyl toluidide (HTMT) (**i**), dopamine receptor agonist quinpirole (**j**) or dopamine receptor antagonist haloperidol (**k**) ($n = 3$, mean and s.d., ns = not significant). **l**, Various nicotinic receptor antagonists have no effect on OPC differentiation. **m**, Benztropine blocks carbachol- and muscarine-induced activation of Notch signalling measured by western blot for intracellular domain of Notch1. (a.u., arbitrary unit, $n = 3$, mean and s.d., $^{*}P < 0.05$, *t*-test). **n**, Naive whole rat brain and rat primary OPCs treated with DMSO (<0.1%) or T3 (1 μM) for 6 days tested for expression of muscarinic receptors and choline acetyl transferase (ChAT) by PCR using gene-specific primers. **o**, Quantification of M1, M2, M3, M4 and ChAT expression by qRT-PCR. ($n = 3$, mean and s.d., expression fold change normalized to OPCs). **p**, OPCs treated with benztropine (25 μM) and pelleted for western blot analysis of total protein. **q**, Carbachol induced a dose-dependent increase in intracellular Ca^{2+} levels, whereas benztropine and atropine (a muscarinic antagonist) dose-dependently blocked carbachol (50 μM) induced calcium influx through antagonism of M1/M3 muscarinic receptors. **r**, Benztropine (13 μM) had no effect on the levels of cAMP. Forskolin is a positive control for increasing intracellular cAMP ($n = 3$, mean and s.d., $^{*}P < 0.05$, *t*-test).

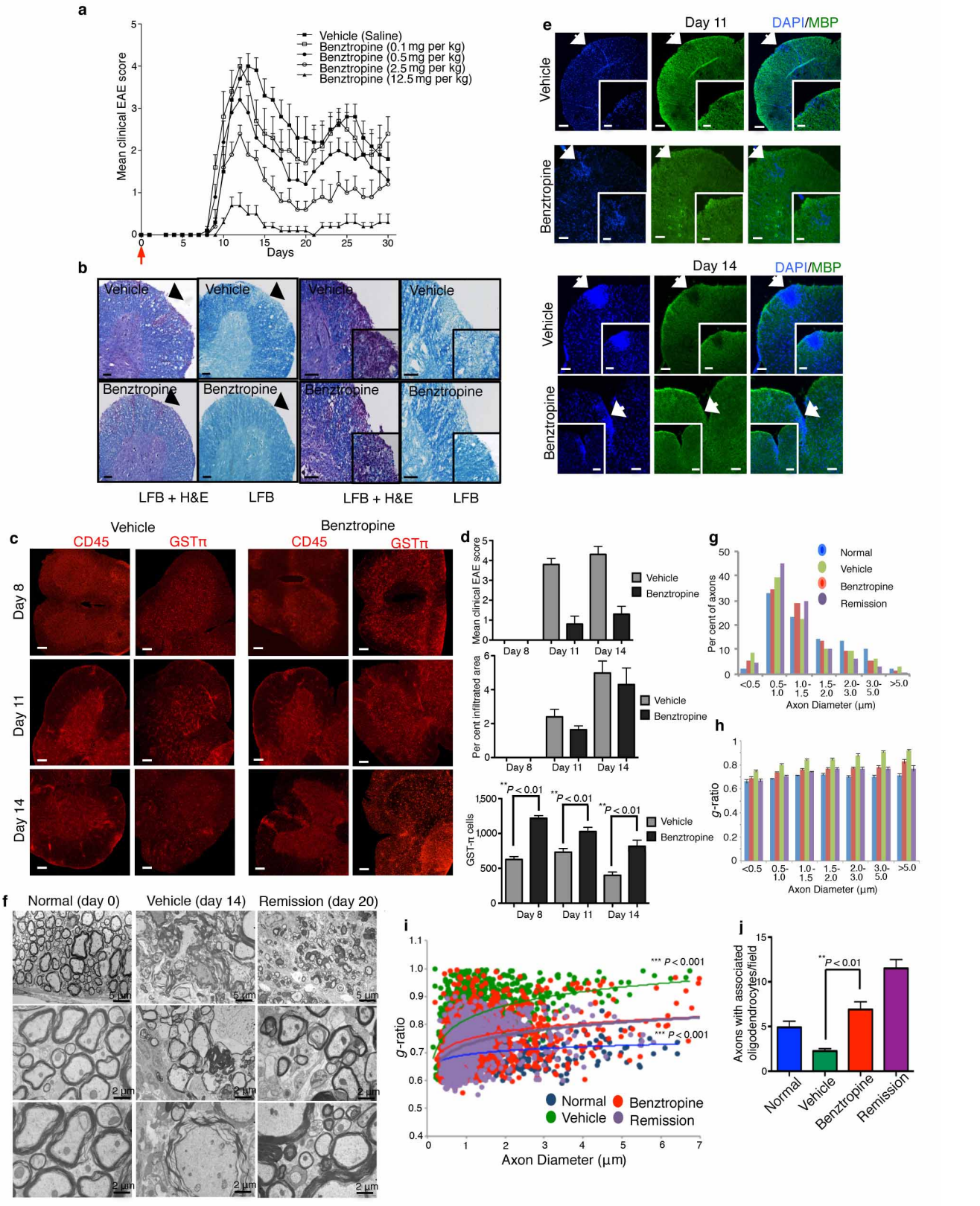

Extended Data Figure 4 | Benztropine dose-dependently reduces clinical severity and induces remyelination in the PLP-induced EAE model. **a**, Clinical severity scores of EAE mice treated with various doses of benztropine in the prophylactic mode ($n = 8$, mean and s.e.m.). **b**, EAE mice treated with benztropine (10 mg per kg) or vehicle in the therapeutic mode and spinal cord sections from mice representative of the average group scores during the relapse phase of EAE stained with Luxol fast blue and H&E, or Luxol fast blue only. Arrows point to regions of lymphocyte infiltration (LFB + H&E) or demyelination (LFB). Scale bars represent 100 μm. EAE mice treated with benztropine (10 mg per kg) or vehicle in prophylactic mode. **c**, Spinal cord sections from mice representative of the average group scores on day 8, 11 and 14 immunostained with antibodies specific to CD45 and GSTπ. **d**, Mean clinical scores of mice at the time of spinal cord isolation and quantification of the infiltrated areas ($CD45^+$) and number of $GST\pi^+$ cells ($n = 8$, mean and s.e.m., $^{**}P < 0.01$, *t*-test). Scale bars, 100 μm. **e**, EAE mice treated with benztropine (10 mg per kg) or vehicle in prophylactic mode and spinal cord sections from mice representative of the average group scores on day 11 and 14, immunostained with antibody specific to MBP. Arrows point to regions of lymphocyte infiltration. Scale bars, 100 μm. **f**, Electron microscopy images showing myelin around axons in normal mice, vehicle-treated mice and mice in remission. Scale bars as indicated. **g**, Analysis of electron microscopy images indicating distribution of axonal diameters measured for 4 groups. **h,** Analysis of electron microscopy images indicating distribution of *g*-ratios of axons for 4 groups. **i**, Scatterplot of *g*-ratios in relation to spinal cord axonal diameters ($n = 1{,}000$, $^{***}P < 0.001$, one-way ANOVA, exponential trend line). **j**, Quantification of the number of axons associated with oligodendrocytes ($n = 25$, mean and s.e.m., $^{**}P < 0.01$, *t*-test). Oligodendrocytes were identified visually by their cytoplasmic processes wrapping around axons.

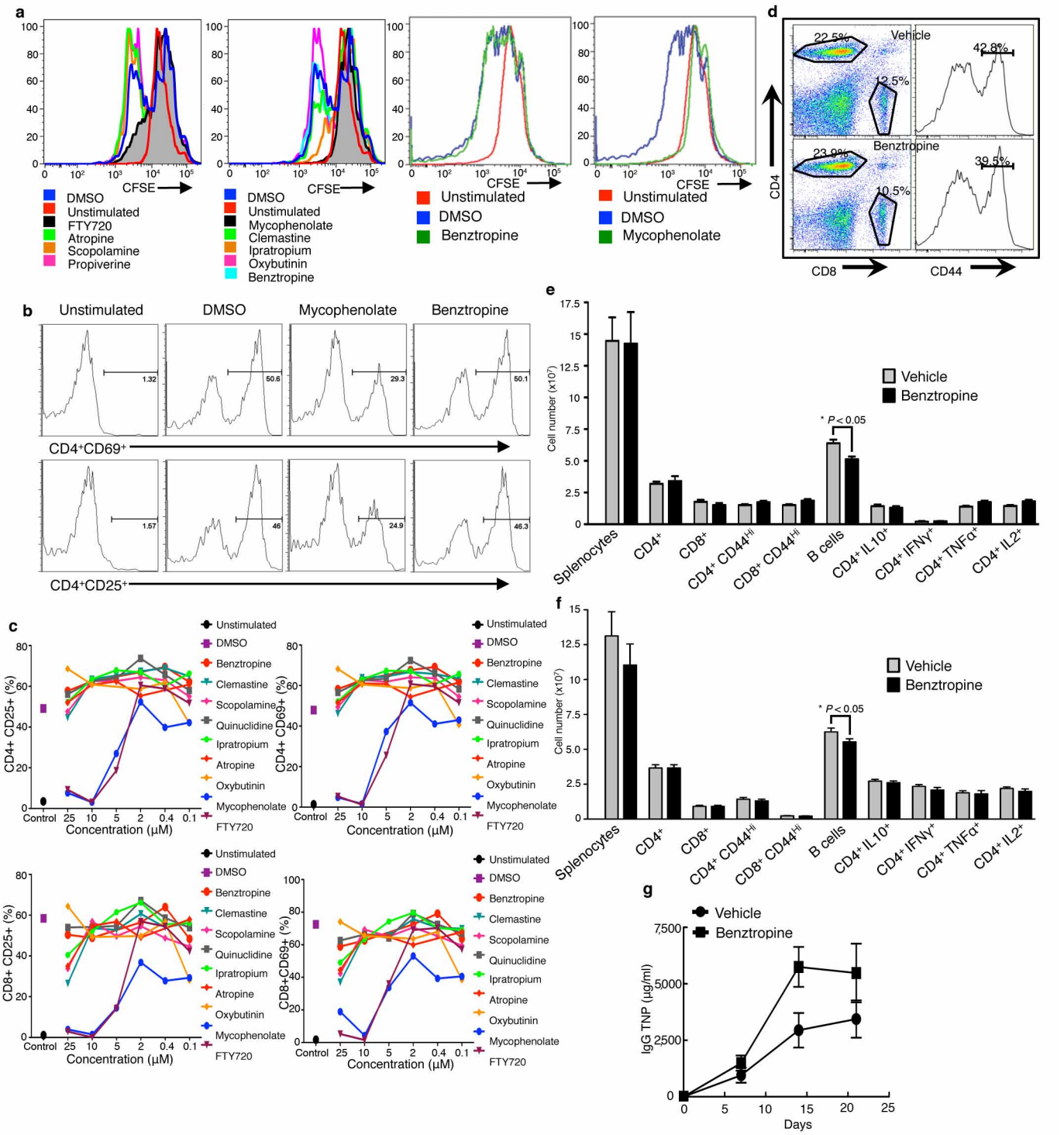

Extended Data Figure 5 | Benztropine has no effect on *in vitro* and *in vivo* immunological responses in EAE mice. **a**, Benztropine and various muscarinic antagonists have no effect on *in vitro* T-cell proliferation measured using carboxyfluorescein succinimidyl ester (CFSE) labelling, whereas mycophenolate and FTY720 suppress T-cell proliferation as determined by the percentage of $CD4^+$ T-cell-gated populations positive for the given marker. **b**, **c**, Various muscarinic antagonists have no effect on T-cell activation as measured by $CD4^+CD25^+$, $CD4^+CD69^+$, $CD8^+CD25^+$ and $CD8^+CD69^+$ cell populations. FTY720 and mycophenolate serve as positive controls for suppression of T-cell activation. **d**, Representative flow cytometry scatter plots show similar numbers of $CD4^+$, $CD8^+$, and $CD44^{Hi}$ cells in spleens isolated from vehicle- and benztropine-treated mice. **e**, **f**, Total splenocytes isolated from benztropine (10 mg per kg) or vehicle treated (14 days in the prophylactic mode) naive SJL/J (**e**) or EAE (**f**) mice analysed for various populations of immune cells and cytokine secretion. Benztropine treatment had no effect on the numbers of total splenocytes, $CD4^+$ T cells, $CD8^+$ T cells, $CD4^+CD44^{Hi}$ T cells and $CD8^+CD44^{Hi}$ T cells. Benztropine treatment showed a minor, but significant decrease in the number of B cells ($n = 5$, mean and s.e.m., $^*P < 0.05$, *t*-test). Benztropine had no effect on cytokine production from $CD4^+$ T cells expressing IL-2, IL-10, TNF-α or IFN-γ. ($n = 5$, mean and s.e.m.). **g**, Benztropine showed no effect on keyhole limpet hemocyanin protein conjugated to 2,4,6-trinitrophenyl hapten (TNP-KLH)-induced T-cell-dependent B-cell response. Mice were injected with TNP-KLH in adjuvant and treated with vehicle or benztropine (10 mg per kg) daily. Serum was isolated at various time points and anti-TNP-IgG levels were measured by ELISA. (3 replicate ELISAs, $n = 5$ mice per group, mean and s.e.m.).

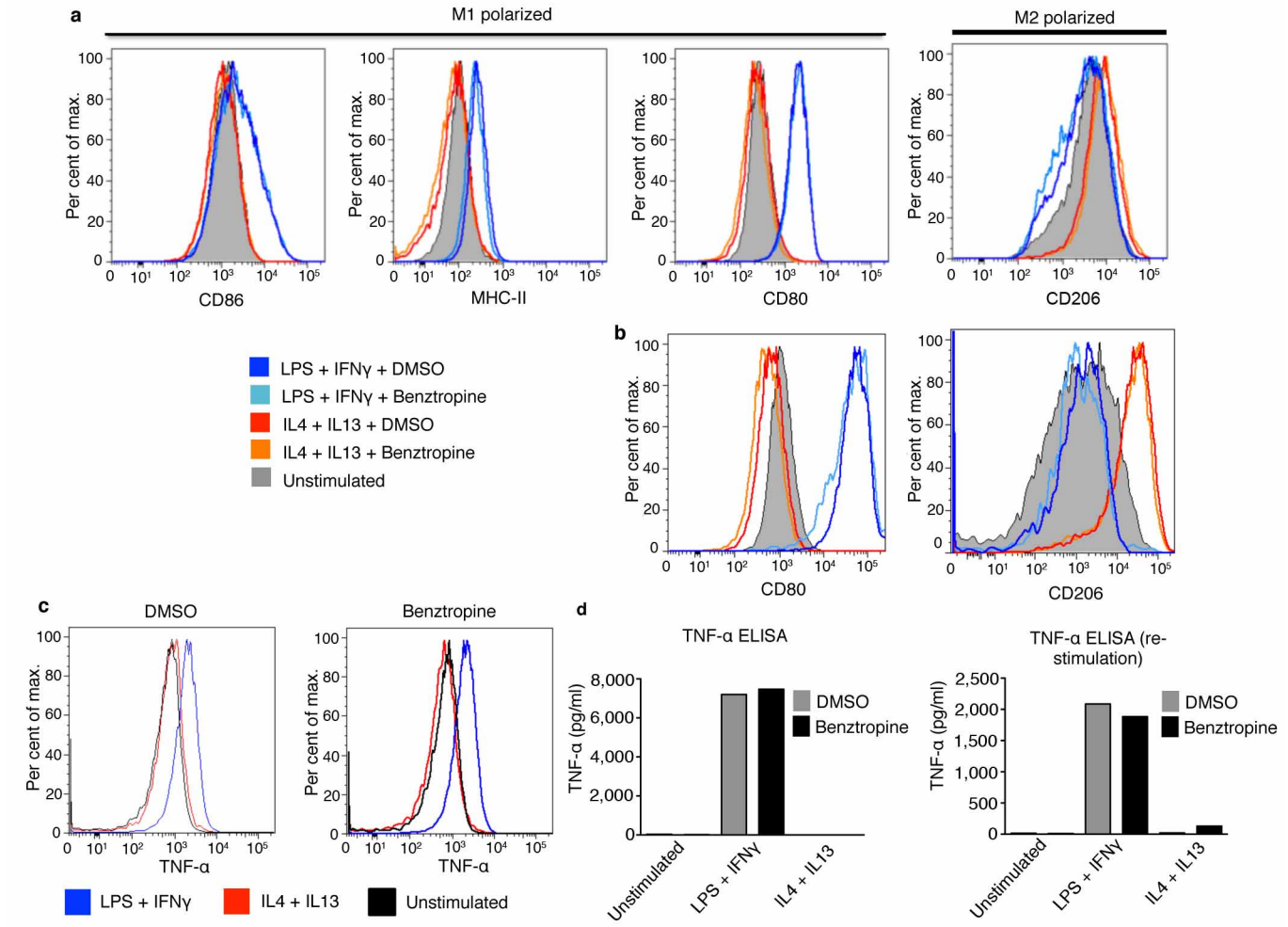

Extended Data Figure 6 | Benztropine does not affect derivation and *in vitro* polarization of macrophages from bone marrow derived monocytes. **a**, Flow cytometry analysis of bone marrow derived monocytes treated *in vitro* with either DMSO (<0.1% v/v) or benztropine (5 μM) for 24 h followed by 24 h treatment with LPS (100 ng ml^{-1}) plus IFNγ (20 ng ml^{-1}) for the expression of M1 markers: CD86, MHC-II and CD80, or 24 h treatment with IL-4 plus IL-13 (20 ng ml^{-1} each) for the expression of M2 marker CD206. **b**, M1/M2 polarized macrophages re-stimulated using either LPS (100 ng ml^{-1}) plus IFNγ (20 ng ml^{-1}) (M1) or IL-4 plus IL-13 (20 ng ml^{-1} each) (M2) for 16 h in the presence of either benztropine (5 μM) or DMSO and analysed for the expression of M1 (CD80) or M2 (CD206) markers by flow cytometry. **c**, **d**, Treatment with LPS (100 ng ml^{-1}) plus IFNγ (20 ng ml^{-1}) induced the expression of the prototypical M1 cytokine TNF-α as detected by intracellular flow cytometry (**c**) and ELISA (**d**) with no significant differences between DMSO or benztropine (5 μM) treated cells (data representative of 2 replicate experiments).

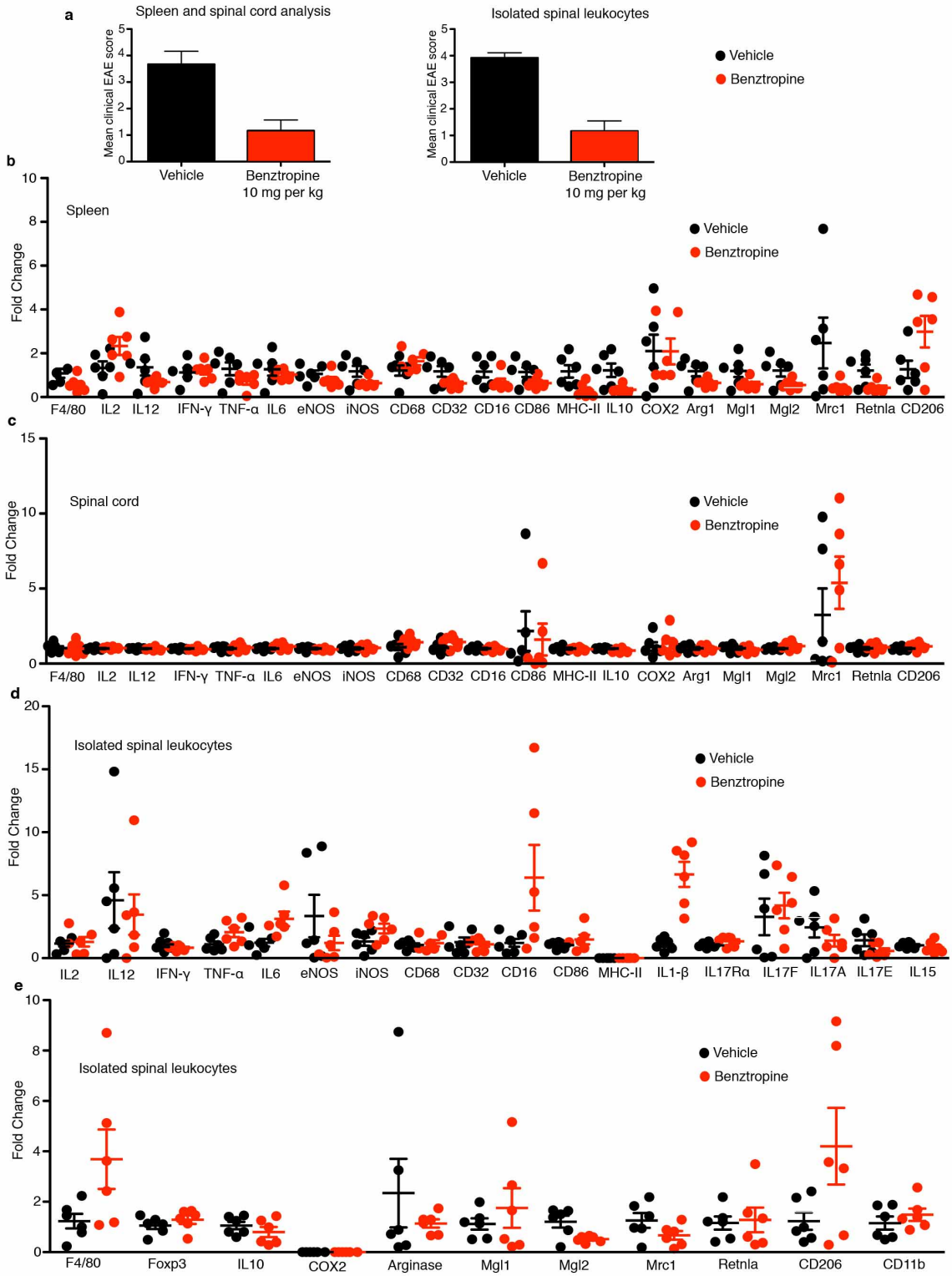

Extended Data Figure 7 | Benztropine does not affect *in vivo* polarization of macrophages in the spleen or spinal cord. EAE mice were treated with benztropine (10 mg per kg) or vehicle for 14 days in the prophylactic mode. **a**, Mean clinical EAE scores for mice treated with vehicle or benztropine ($n = 6$, mean and s.e.m. for spleens and spinal cords, $n = 12$ for isolated spinal leukocytes analysis). **b**–**e**, Spleens and spinal leukocytes were isolated from the mice as described in Methods. Total RNA was isolated, reverse transcribed and gene expression was measured by qRT–PCR. Expression for each marker was normalized to the average gene expression of the vehicle group. No significant differences were observed in the expression of markers of macrophage polarization in the spleen (**b**), whole spinal cords (**c**) and leukocytes (**d**, **e**) isolated from spinal cords ($n = 6$ mice per group for spleens and spinal cords, $n = 12$ mice per group ($n = 6$ for qRT–PCR) for spinal leukocytes analysis. Error bars represent s.e.m.).

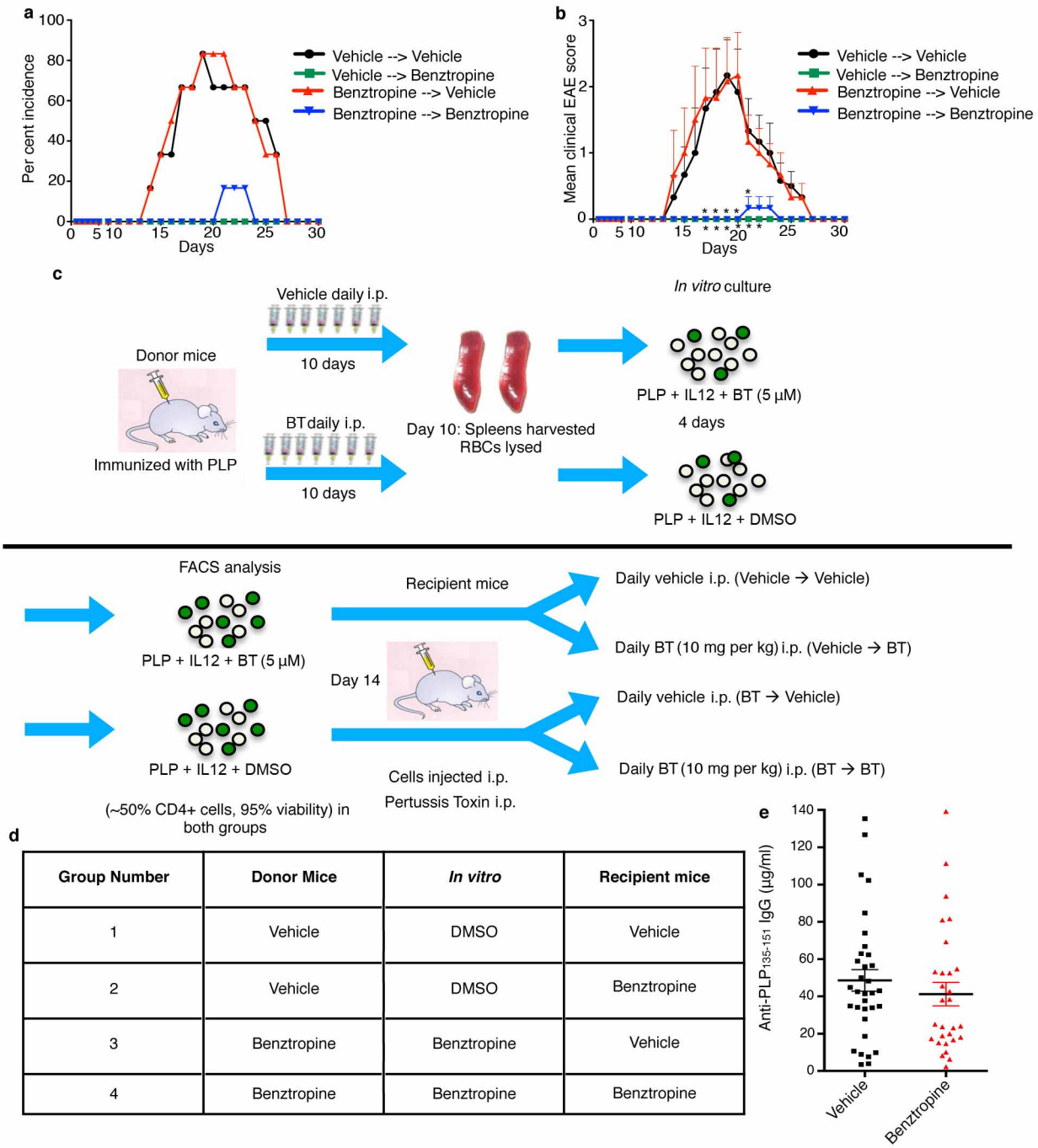

Group Number	Donor Mice	*In vitro*	Recipient mice
1	Vehicle	DMSO	Vehicle
2	Vehicle	DMSO	Benztropine
3	Benztropine	Benztropine	Vehicle
4	Benztropine	Benztropine	Benztropine

Extended Data Figure 8 | Benztropine does not affect clinical severity in an adoptive transfer model of EAE. **a**, **b**, Incidence of adoptive transfer of EAE (**a**) and mean clinical EAE scores (**b**) in mice injected with splenocytes isolated from benztropine- or vehicle-treated donor groups. T cells obtained from either benztropine- (BT, 10 mg per kg) or vehicle-treated donor EAE mice and further expanded in the presence or absence of benztropine (5 µM) were able to adoptively transfer EAE to naive recipient mice. Benztropine-treated recipient mice showed little to no clinical symptoms of EAE compared to vehicle-treated recipient mice, whether injected with benztropine- or vehicle-treated donor splenocytes ($n = 6$ mice, mean and s.e.m., $^*P < 0.05$, *t*-test). **c**, Schematic for the adoptive transfer EAE model. **d**, Table showing various groups and treatments. **e**, ELISA for anti-PLP IgG shows equivalent PLP response in donor mice treated with either vehicle or benztropine ($n = 30$, mean and s.e.m).

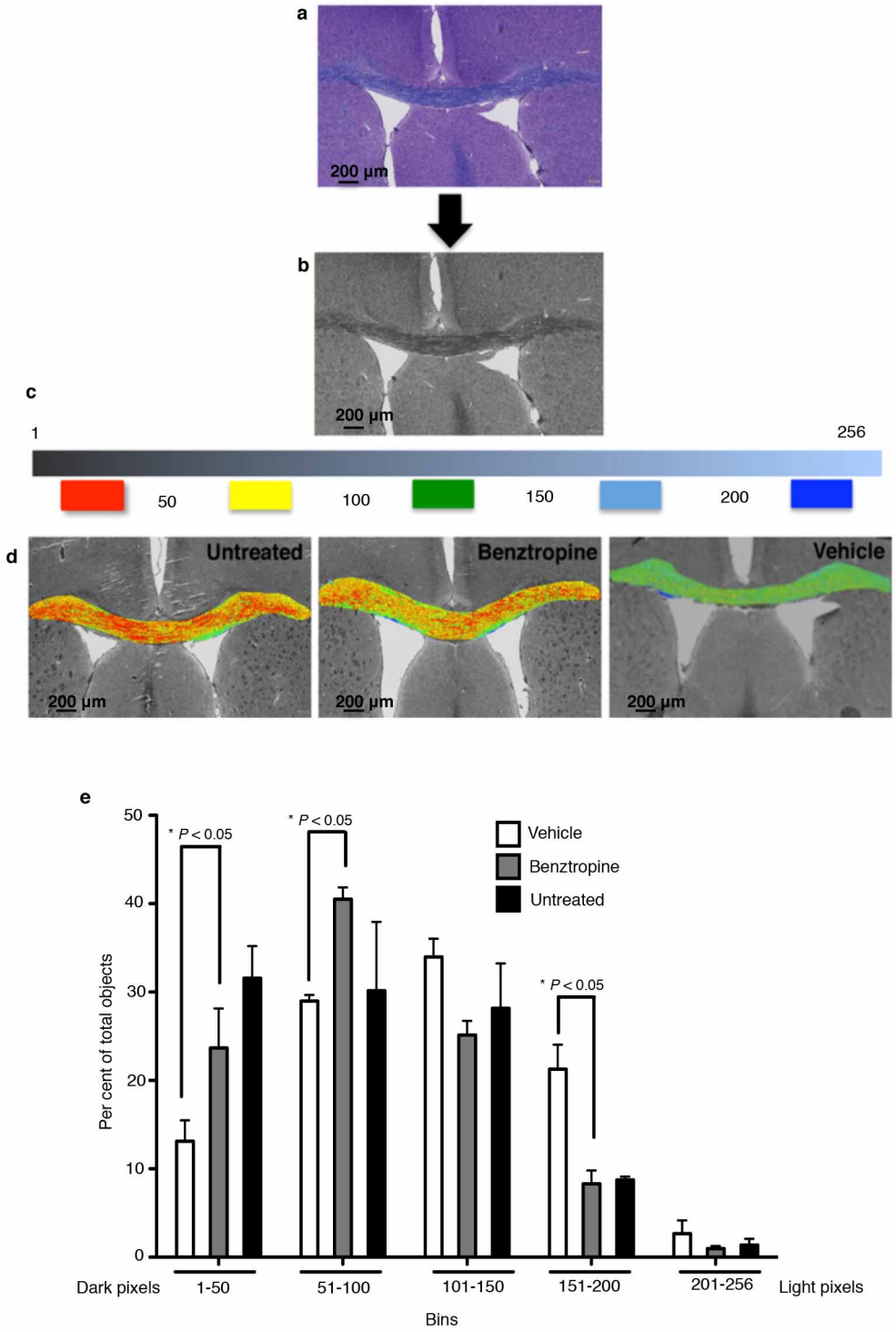

Extended Data Figure 9 | Quantification of myelin staining in the cuprizone model. **a**, Luxol fast blue (LFB) and H&E staining was performed on sections from the corpus callosum region of brains isolated from mice treated either with benztropine (10 mg per kg) or vehicle after 7 weeks of exposure to cuprizone. **b**, Images were converted to a 256 shade grey scale. **c**, The 256 shades of grey were divided into 5 bins of 50 shades each (1–50, 51–100, 105–150, 151–200 and 201–256). Number of objects in the corpus callosum region in each bin were counted using Image-Pro plus. **d**, Representative images of Image-Pro rendering of the quantification of objects in each bin. **e**, Quantification of Luxol fast blue staining on week 2 shows an increase in the darker pixels (1–50 and 51–100) with benztropine treatment along with corresponding reduction in the number of lighter pixels (151–200). Six images per mouse were analysed and four mice per group were used at each time point (mean and s.d., $*P < 0.05$, *t*-test). Scale bars, 200 µm.

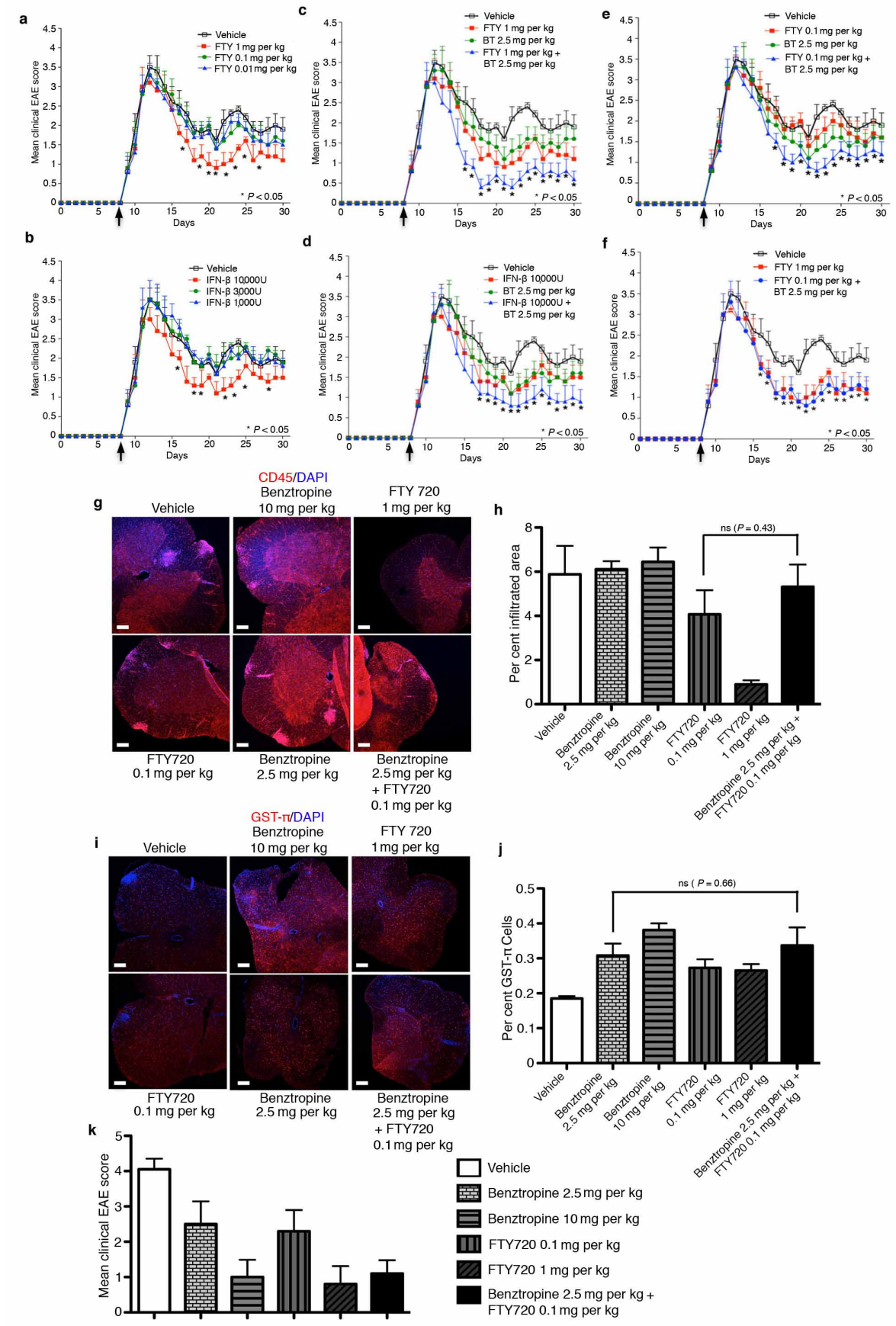

Extended Data Figure 10 | Effect of the addition of benztropine to interferon-β and FTY720 treatments. **a**, **b**, EAE severity scores for mice treated with various doses of FTY720 (**a**) or interferon-β (**b**). **c**, Mice treated therapeutically with FTY720 (1 mg per kg) in combination with a sub-optimal dose of benztropine (BT, 2.5 mg per kg) show significantly decreased clinical severity compared to FTY720 (1 mg per kg) or benztropine (2.5 mg per kg) alone. **d**, EAE mice treated with interferon-β (IFN 10,000 U per mouse) in combination with benztropine (2.5 mg per kg) show significantly decreased clinical severity compared to interferon-β (IFN; 10,000 U per mouse) or benztropine (2.5 mg per kg) alone. **e**, EAE mice treated with a tenfold lower dose of FTY720 (0.1 mg per kg) in combination with benztropine (2.5 mg per kg). **f**, EAE mice treated with a tenfold lower dose of FTY720 (0.1 mg per kg) in combination with benztropine (2.5 mg per kg) show clinical severity comparable to optimal dose of FTY720 (1 mg per kg) ($n = 8$ mice per group, mean and s.e.m., $^{*}P < 0.05$; *t*-test). **g**, **i**, Spinal cord sections from EAE mice treated with the indicated drug(s) for 14 days in the prophylactic mode and immunostained for CD45 (immune cells) and GSTπ (oligodendrocytes) showing infiltration (**g**) and oligodendrocytes (**i**). **h**, **j**, Quantification of the number of $CD45^{+}$ (**h**) and $GST\pi^{+}$ (**j**) cells showing a decrease in infiltrating cells with FTY720 treatment and an increase in oligodendrocytes numbers with benztropine treatment and synergy between benztropine (2.5 mg per kg) and FTY720 (0.1 mg per kg) ($n = 5$, mean and s.e.m., ns, not significant). Scale bars, 100 μm. **k**, Mean clinical EAE scores for mice at the time of spinal cord isolation ($n = 8$, mean and s.e.m).